https://doi.org/10.5194/egusphere-2023-1474
Preprint. Discussion started: 22 August 2023


# UV solar radiation climatology and its behaviour during events of influence of the Antarctic ozone hole over south of Brazil

Bibiana Culau Lopes[1], Damaris Kirsch Pinheiro[1], Hassan Bencherif[2], Gabriela Dornelles Bittencourt[1], Lucas Vaz Peres[3], Jean-Maurice Cadet[2], Thierry Portafaix[2], Nathalie Tissot Boiaski[1].

[1]Department of Meteorology, Federal University of Santa Maria, Santa Maria, RS, 97105-900, Brazil
[2]University of Reunion Island, LACy, UMR8105, Saint-Denis, Réunion, France
[3]Federal University of Western Pará, Santarém, PA, Brazil

*Correspondence to*: Bibiana Culau Lopes (bibianaclopes@gmail.com)

**Abstract.** Ultraviolet solar radiation that reaches the surface of the Earth has a very important role in the energy budget of our planet, although at certain amounts of exposure it can be harmful not only for human health, but animals and plants. Brazil is a tropical country receiving high intensity of UV radiation mostly of the year. UV radiation, specially UV-B is mainly absorbed in the ozone layer, changes in ozone content or ozone distribution directly affects UV radiation attenuation, so that surface UV. Ozone hole is characterized by an intense ozone depletion in the stratosphere in Antarctic region, happening during spring in the south hemisphere. There is evidence of poor-ozone air masses detachment from polar vortex and reaching mid-latitude regions, such as South of Brazil. Those air masses cause impact on the regions which they act due to low ozone content, allowing more radiation to reach the surface. UV index data from a Brewer Spectrophotometer (MKIII #167), located in south of Brazil, in the Southern Space Observatory (29.42° S, 53.87° W) was analysed with data collected between 2005 and 2017. Ground data was compared to satellite-derived from OMI/Aura, resulting in a correlation coefficient of 0.95%. The climatology of Brewer data was done, analysing seasonal and interannual variability. Wavelet analysis showed the influence of ENSO, QBO and solar cycle on the variability of UV index. The results show a typical seasonal behaviour of UV Index, reaching extreme during summer season. Events of secondary effects of Antarctic ozone hole, identified between 2005 and 2016 (Bittencourt, 2018), were selected and the behavior of UV index and UV-B non-weighted during those events were studied. All ten events studied showed a significant increase in UV radiation at the days of events, the majority resulted in an increase of 4% of UV index for each 1% ozone total column decrease. One specific event was described in detail due to the major ozone depletion. Occurred in October 2016, ozone depletion was of almost 20% while UV index increased 88% in relation to the climatological mean, raising the concern with public health regarding excess exposure to UV radiation.

## 1 Introduction

Solar radiation that reaches Earth's atmosphere and surface is one of the most important elements in climate. The amount of energy that is absorbed and reflected by the atmosphere and surface of the Earth contributes for the energy balance of our planet. The energy budget includes many processes of scattering, absorbing and reflection of energy on the way between the

https://doi.org/10.5194/egusphere-2023-1474
Preprint. Discussion started: 22 August 2023


sun and the surface of the Earth. Ultraviolet radiation (UVR) (from 100 to 400 nm) is in a region of the electromagnetic spectrum that do not corresponds to the visible region, in other words, the human eye is not sensitive to light in this band, between 400 nm and 780 nm (Liou, 2002; Wuebbles, 2015). Since it reaches the surface, UVR is extensively studied due to its biological effects on human health, fauna and flora (WHO et al., 1994). It is divided in three wavelength bands that are differently affected by the atmosphere. UV-C, from 100 to 280 nm, does not reach the surface because it is totally absorbed by ozone and oxygen in the atmosphere, UV-B, from 280 to 320 nm, is highly absorbed by the ozone layer, so it partly reaches the surface, and finally UV-A, from 320 to 400 nm which is weakly absorbed by the atmosphere so, it reaches the surface with more intensity (WHO et al., 1994). The attenuation factors that affect UV radiation include geometrical aspects, such as Sun-Earth distance and solar zenith angle, the variable aspects are scattering by molecules, scattering and absorption by aerosols, surface albedo, and scattering and reflection by the clouds. Specifically, the clouds can be of great influence in UV radiation. Depending on the cloud cover the UV can suffer great attenuation, on the other hand the reflection by some sort of clouds can also increase UV radiation (Seckmeyer et al., 1996; Foyo-Moreno et al., 2003). Normally UV-B and UV-A account for approximately 3% of the total solar radiation, considering a scenario of total clear sky condition. The amount of clouds can cause great variability in the UV radiation. Different sky conditions and the types of clouds can reduce up to 79% UV-B radiation at the surface (Grant and Heisler, 2000; Schafer et al., 1996). Moreover, one of the most important attenuating factors of UVR is the ozone (O3). Ozone layer works as a shield due to the absorption of UVR by ozone molecules, in this reaction ozone absorbs UV radiation causing the photo-dissociation of ozone molecule and resulting in O2 and O. Therefore, the amount of UV radiation absorbed by the ozone layer is directly dependent of ozone concentration (Wuebble, 2015). Regarding to this matter, ozone depletion and its effects in UV radiation intensities on Earth's surface have been widely studied in different parts of the globe by many research groups (Pfeifer and Besaratinia, 2012; Wang et al., 2012; Rozema et al., 1997; Cadet et al., 2005, García-Huidobro, et al., 2017, Cadet et al., 2017; Lamy et al., 2021; du Preez et al., 2019).

The region of the tropics is where most of ozone is formed, due to much stronger intensity of solar radiation. And because of the same reason, in this region there is an upwelling circulation driven by the hot air masses that carry ozone. The Brewer-Dobson circulation is responsible for ozone transport between stratosphere and troposphere at the hemispherical scale. Risen air masses, in tropical regions loaded with gases like ozone, reach tropopause and are horizontally distributed in poleward directions. Air masses are stronger in direction to winter pole, then those masses descend on the polar vortex (Flury et al., 2013).

During winter in Antarctic region, the polar vortex is formed with a very strong jet stream, gases carried with the Brewer-Dobson circulation descend on the top of the vortex. In the beginning of spring solar radiation reacts with gases trapped in polar vortex, including chlorine, fluorine and carbon, the CFC's. Those compounds react with ozone destroying the molecules and strongly reducing its concentration in the region. Ozone total column can decrease lower than 220 DU during the period of Antarctic ozone hole. Throughout the spring, polar vortex weakens and air masses from its edges get released and travel mostly reaching mid-latitude regions (Douglass et al., 2014; Hofmann et al., 1997; Marchand et al., 2005).

https://doi.org/10.5194/egusphere-2023-1474
Preprint. Discussion started: 22 August 2023


Except, on the years of 2020, 2021 and 2022 an odd behavior was observed, instead of polar vortex weakening and the ozone hole begin to decline, it persisted in its maximum until de end of November and then finally closed only in the end of December, being classified as one of the largest since 1979 and the longest-lived. In 2021 the ozone hole was even largest, the eight-larges, on record, and lasted few days less than the one from previous year. During October of 2020 and 2021 ozone loss saturation profiles showed near-zero ozone between 14-21 km layer under the vortex (Johnson et al., 2023). The next year followed the same pattern, the beginning of the season was typical but the Antarctic ozone hole was finally closed only mid-December. Many meteorological factors can have contributed to this atypical behavior, such as the persistent and cold conditions of the polar vortex, since the ozone hole tends to increase with a stronger polar vortex (Copernicus, 2023).

As reported by Kirchhoff et al. (1996), ozone-poor air masses reach south of Brazil, specifically region of Santa Maria. A drastic and fast drop in ozone column was identified, being attributed to Antarctic ozone hole secondary effects, since trajectory analysis confirmed air masses with Antarctic origin, at 20 to 25 km, over Santa Maria region on the days of low ozone. A series of events of secondary effects of Antarctic ozone hole was identified in the same region in the following years by Peres (2016) and Bittencourt (2018).

Ozone distribution on the stratosphere is also influenced by the Quasi-biennial circulation (QBO) and Events of El Niño Southern Oscillation (ENSO) which ends up affecting UV radiation incidence (Herman, J. et al, 2000; Manatsa and Mukwada, 2015; Zhang et al., 2015). Depending on the QBO phase, it acts strengthening or weakening Brewer-Dobson circulation, transporting more or less ozone concentration poleward. ENSO also cause great influence on UV radiation intensity because during El Niño phase precipitation tends to increase significantly while on the La Niña phase the opposite tends to occur, causing drought on the region of study (Cavalcante et al., 2009). Solar cycle occurs every 11 years approximately, it affects the activity on solar surface and varies from solar minimum, less activity on the surface of the sun, to solar maximum, more activity, as sunspots. QBO phase from east during solar maxima is related with higher UV index than UV index during QBO from west, between 15 and 50 hPA (Elias and Zossi de Artigas, 2003). With regard to UV radiation, it contributed for the evolution of plants and human life, it is also a source of vitamin D, which is an important nutrient for the skeleton, bone metabolism, it has positive effects in the immune system, among many other benefits. The deficiency in vitamin D can contribute for osteoporosis in adult life (Rozema et al., 1997; Holick, 2008; Engelsen, 2010). Despite of the fact that UV radiation is essential for nature, the attenuation of UV-B is also extremely important for all living beings on the surface because of its negative effects of excess exposure. Plants exposed to excessive UV radiation provoke modifications in order to adapt, which can cause DNA damage. It causes vulnerability to zooplankton, increasing mortality of its communities in water bodies (Ries et al., 2000; Al-Aidaroos, 2014), also UV radiation can increase oxygen consumption by fish in sea-water. This associated with high temperature can affect its metabolism (García-Huidobro, et al., 2017). The continuous excess of exposure of humans to UV radiation, specifically UV-B, cause DNA lesions that lead to DNA mutations, with potential to the development of skin cancers, including melanoma, which is considered to be one of the most lethal form of skin cancer, because this type of tumour is highly resistant to the treatment (Pfeifer and Besaratinia, 2012). There are issues related to eye damage due to solar UV radiation, such as cataracts, photo-conjunctivitis and muscular degeneration (Wang et al., 2012). The most immediate effect

https://doi.org/10.5194/egusphere-2023-1474
Preprint. Discussion started: 22 August 2023


of solar UV radiation can be perceived is the erythema, it is an acute injury, or the redness on the skin caused by the time of solar exposure.

Based on the health issues regarding to solar UV radiation exposure, it was created the UV Index, which is a standard indicator of UV levels, so the population can be aware of the amount of radiation that they are being exposed to. Thus, it was created intending to be a tool of information for population. It was adopted in 1994 by the World Health Organization and World Meteorological Organization (Wang et al., 2014; Fioletov et al., 2010). The scale starts in zero, until 2, represented by the colour green, it indicates that the UV index is low and there are no safety measures needed. From 3 to 5 it is represented by the colour yellow indicating that index is moderate and the colour orange indicates an UV index between 6 and 7, it indicates high index, on these levels some measures of safety must be taken such as seek for shade, specially between midday and mid-afternoon, when the sun is at its zenith, one should wear sunscreen and sunglasses when going outside. A very high level is represented by red and the index is from 8 to 10, above 11 the index is considered extreme and in the scale of colours is represented by purple, at this levels of UV index extra protection is needed, besides the sunscreen, wear protective clothing and wide-brimmed hat (EPA, 2019). Brazil is a tropical country and its levels of UV index can easily reach extreme values specially in certain periods of the year and region. The main part of the country is exposed to high levels of UV index mostly of the year. The south region shows a decrease of UV index during winter season with an increase tendency during spring and extreme levels during summer (de Paula and Pires, 2013).

This study aimed to investigate the variability of UV index in the south region of Brazil with UV radiation data measured with a Brewer Spectrophotometer, between the years of 2005 and 2017 and UV index retrieved from OMI/Aura satellite for the same period. Comparison of both measurements was done and climatology of ground measurement was obtained showing seasonal and interannual behaviour of UV radiation on the region. It was considered data from all sky conditions and, in parallel, clear sky days were analysed, considering the influence of clouds in solar radiation intensity. Interannual variabilities were investigated by the use of wavelet analysis.

Ten events of low-ozone air masses were analyzed with regard to UV radiation intensity in Santa Maria region, in South Brazil. UV radiation parameter used were UV index and UV-B non-weighted and as ozone parameter it was accounted ozone total column. One event occurred on October, 2016 was thoroughly described due to its significant drop in ozone content and consequently extreme UV index reached.

## 2 Methodology

### 2.1 Ground measured UV index data

Ground measurements were taken in the south region of Brazil where the National Institute of Space Research (INPE) has one of its research centres, the Southern Space Observatory (SSO). It is located in the city of São Martinho da Serra, the geographic coordinates of the site are latitude 29° 26’ 24” South and Longitude 53° 48’ 38” West, at 488 meters above sea level. The Brewer spectrophotometer is placed on a platform and connected to a station where all collected data is stored as well as the

https://doi.org/10.5194/egusphere-2023-1474
Preprint. Discussion started: 22 August 2023


configurations of the equipment are set. Measurements of solar UV radiation were collected with a Brewer Spectrophotometer, MKIII#167 (Kipp Zonen). The spectrophotometer is an optical instrument that measures the intensity of attenuation of solar ultraviolet radiation, in five different wavelengths and in the spectrum of absorption of atmospheric ozone and sulphur dioxide. It also measures the intensity of UV-B on the surface, the Total Column Ozone and Total Column Sulphur Dioxide. The instrument accounts with a double monochromator system which provides good accuracy in spectral intensity profiles of UV radiation, in a spectral range of 286.5 nm to 363 nm. The equipment is composed by the spectrophotometer, a solar tracker and the computer system that allows to set configurations for measurements and also stores all data collected. The solar tracking system includes an algorithm for azimuth and zenith angles calculation of the sun and the moon from equipment's location. Information as geographic co-ordinates, time and date in GMT are needed for calculations. The solar radiation enters directly in a side window and is directed through the optical system where the solar zenith angle is identified providing measurements of direct solar radiation (SCI-TEC, 1999). Data collected of the measurements from Brewer spectrometer consist in raw data and they are all stored on hard disk drive of the computer connected to Brewer. The results are later processed in Brewer's software. Measurements of UV are done every 30 minutes from approximately 7 am, local time and the last measurement is done around 6 pm also local time, the systems use GMT time. UV files generated during measurements are analysed in the software developed by Ing Martin Stanek (Solar and Ozone Observatory of CHMI/International Ozone Service). UV Data can be processed using filters to obtain UV radiation spectrally weighted for biological effective UV, in this case the action spectrum is given by CIE Erythema (mW/m2). The UV index is also accounted at the moment of each measurement. The UV radiation data can also be processed without filters to obtain the measurements of UV-B non-weighted.

Regarding ozone total column data used in the study of UV radiation behaviour during events of secondary effects of Antarctic ozone hole, it was collected with Brewer and OMI overpass data was used in order to fill the missing data due to days without measures from the Brewer instrument (OMI-ERS2/NASA, 2017).

### 2.2 Clear-sky day selection

Data analysis in the Brewer's software provides the plot of the daily UV scan. UV measurements of clear-sky days result in a very smooth bell-shaped curve. Clouds normally cause an attenuating affect in the UV and end up changing the shape of the curve with spikes. The clear-sky days were, firstly selected through visual observation of the curve shape where its highest pick is around noon time, when the sun is stronger. Then, days selected as clear-sky were reviewed with cloud fraction and images from an All sky camera. Total cloud fraction data and images from an All-sky camera were considered in this study to corroborate with clear-sky days selected. The All-Sky Camera (EKO Instruments) used is digital composed by fisheye lens and with a field of view of 180°, protected with a water prof box and heating system to protect from weather and temperature changes (Luiz et al., 2018). The Total Sky Imager processes the image obtained and the ratio of cloud in the sky is estimated based on thin cover and opaque cover of clouds. Cloud fraction represents the cloud coverage, it is calculated with a software based on the image and type of cloud (Slater et al., 2001).

https://doi.org/10.5194/egusphere-2023-1474
Preprint. Discussion started: 22 August 2023


### 2.3 Satellite-derived UVR data

Satellite data used in this study are derived from Ozone Monitoring Instrument (OMI), a spectrometer aboard Aura satellite, part of NASA's Earth observing System. It was launched in 2004 and is part of an atmospheric chemistry mission. Specifically, the OMI sensor, since 2004, collects data regarding to ozone layer, aerosol sources and solar UV radiation (OMI, 2012). Therefore, UV index data were retrieved from GIOVANNI platform (https://giovanni.gsfc.nasa.gov/giovanni) that contains data of UV index from OMI/Aura available for download. All sky UV index and clear-sky UV index were used to be compared with ground-based data, for the period from 2004 to 2017.

### 2.4 Methods of analysis

Ground based data series was analysed considering all-sky conditions and also, separately, considering only days of clear-sky, according to the selection of clear-sky days criteria as described previously. Clear-sky conditions dataset from Brewer was compared to UV index data from OMI, and the correlation coefficient (r) was calculated (Equation 1) to observe their similarities and the daily bias to understand the differences between them. The correlation between satellite and ground measurements of UV index was done with a data series from 2005 to 2017, since satellite data is available from the end of 2004.

Eq. (1):

$$r = \frac{\sum_m \sum_n (Bre_{mn} - MeanBre)(OMI_{mn} - MeanOMI)}{\sqrt{((\sum_m \sum_n (Bre_{mn} - MeanBre)^2 (\sum_m \sum_n (OMI_{mn} - MeanOMI)^2)}}, \quad (1)$$

where the root means square error (RMSE) was calculated (Equation 2), it is a measure of the difference between satellite and Brewer UV index values. And the mean absolute bias error (MABE) (Equation 3) was found to ensure the good result of correlation. Bias (Equation 4) to see the difference between the two datasets and the dispersion of bias was determined through standard deviation (Equation 5)

Eq. (2):

$$Bias\ (\%) = \frac{100}{N} \sum_{i=1}^{N} \frac{OMI - Bre}{Bre}, \quad (2)$$

Eq. (3):

$$RMSE = \sqrt{\frac{1}{N-1} \sum_{i=1}^{N} (OMI - Bre)^2}, \quad (3)$$

Eq. (4):

$$MABE = \frac{100}{N} \sum_{i=1}^{N} \frac{|OMI - Bre|}{Bre}, \quad (4)$$

Eq. (5):

$$Standard\ Deviation = \sqrt{\frac{1}{N-1} \sum_{i=1}^{N} ((OMI - Bre) - Bias)^2}, \quad (5)$$

https://doi.org/10.5194/egusphere-2023-1474
Preprint. Discussion started: 22 August 2023


Climatology of ground-based UV index was done for both data sets all-sky and clear-sky conditions using the same criteria. Daily, monthly means of the whole period and the daily mean by season were calculated. Equation (6) corresponds to the calculation of the mean, whereas Equation (7) was used to calculate standard deviation.

Eq. (6):

$$\mu = \frac{1}{N}\sum_{i=1}^{N} UVindex_i, \quad (6)$$

Eq. (7):

$$Std = \sqrt{\frac{1}{N-1}\sum_{i=1}^{N}|UVindex_i - \mu|^2}, \quad (7)$$

Interannual variability were investigated by the use of wavelet analysis. Those tools are very useful to observe variability patterns and also point variation that may occur in a time series (Torrence and Compo, 1998). Reconstructed time series, from 2005 to 2017, with Brewer and OMI measurements of UV index on clear-sky days, was used in this study. The anomaly was obtained by the subtraction of the monthly climatological mean from the daily value of UV index. The wavelet transformed – Morlet was applied to the anomaly data series. This method of transformed wave consists in a plane wave modulated by a Gaussian function, represented by Equation (8), where: 0 is the non-dimensional frequency; is the non-dimensional time parameter.

Eq. (8):

$$\psi 0\,(\eta) \;=\; \pi\,1\,4\;\mathrm{e}\;\mathrm{i}\;\omega 0\;\eta\;\mathrm{e}\;-\eta\;2\;2, \quad (8)$$

Considering the discrete time series (Xn), with a fixed time spacing (t) and n=0,. . . ,N-1, the continuous wavelet transform is in Equation (9), where (*) is the complex conjugate and s is the period (wavelet scale). The global wavelet spectrum (Equation 10) allows to calculate the unbiased estimation of the true power spectrum of the time series, through the calculation of the average wavelet spectrum over a period.

Eq. (9):

$$W_n(s) = \Sigma_{n'=0}^{N-1} X_n \Psi * \left[\frac{(n'-n)\Delta t}{s}\right], \quad (9)$$

Eq. (10),

$$W^2(s) = \frac{1}{N}\,\Sigma_{n=0}^{N-1}\,|W_n(s)|, \quad (10)$$

Wavelet represents functions in different scales and time (Daubechies, 1992). The wavelet is composed by the power spectrum, where the edges are closed by a ‘U’ curve called cone of influence, where there is a 95% confidence level. The global wavelet spectrum contains the most significant values and also indicates 95% confidence level in the plot, showing the result statistically significant. In order to determine the measure of relative power for the anomaly time series, wavelet power spectrum was normalized by |Wn (s) |2 σ2.

https://doi.org/10.5194/egusphere-2023-1474
Preprint. Discussion started: 22 August 2023


### 2.4 Events of secondary effects of Antarctic ozone hole

A series of events of secondary effects were identified by Peres et al. (2016) and Bittencourt et al. (2018) between 2005 and 2016 and a methodology for identification of those events was described in the same studies. Analysing ozone total column, potential vorticity field and backward trajectories of air masses, from HYSPLIT model (Rolph et al., 2017) is possible to identify the events. The daily mean of ozone total column lower than the climatological monthly mean is the first step, followed by the absolute potential vorticity in isentropic surfaces, as it acts like a mass tracker where potential temperature is conserved and used as horizontal coordinate (Hoskings et al., 1985). The origin of the air masses is confirmed through four different potential temperatures (475 K, 530 K, 600 K and 700 K) obtained using daily mean data from ECMWF (Semane et al., 2006) of stratospheric fields. After identifying the events meteorological fields of troposphere dynamics were done in order to observe its behaviour prior, during and days after the events (Bittencourt et al., 2018). Usually the events tend to be persistent for a couple of days after its arrival on the region, until ozone total column is recovered. Besides that, in some events it was cloudy at day of event, shading the UV radiation increase at this day, for this reason, in some cases, it was selected a day after the day of event when UV index reached higher values, instead of the specific first day of event. A total of 10 events were selected to be studied in this research considering availability of UV radiation data from Brewer. The events occurred between 2005 and 2016, being seven events with its first day happening with a clear sky condition and seven events with cloudy sky condition in its first day. Ozone total column and UV index from Brewer spectrophotometer were used in this study. Eventual gaps in ozone data set was filled using data retrieved from OMI sensor. With daily values of ozone total column and maximum daily UV index from Brewer, the climatological monthly mean was obtained for both ozone and UV index. Those daily values of ozone total column and UV index were plotted considering 10 days before and 10 days after the day of event, in order to visualize UV index response to the decrease in ozone total column. Satellite images of each event studied were included with the intention to observe cloud cover in the region. Satellite images GOES 13 are from thermal infrared channel, it helps in analysis of troposphere, identifying the systems influencing the region of study (CPTEC, 2017).

## 3 Results and discussion

### 3.1 Comparison between ground measurement and satellite data

UV index from OMI is measured once a day and the overpass time is around noon time. The satellite started in 2004, even with the measurements being ongoing until the present day, they were considered in this study until 2018. UV index from OMI (orange dots) and from Brewer (blue dots) were overlap in Figure 1. All-sky measurements are depicted in the upper panel, while clear-sky values are given in lower one. Visually, the comparison between UV index measured with Brewer and UV index from OMI satellite show a similar behaviour of UV index, well representing the seasonal pattern along the years. Correlation between the two sources of measurements, satellite and ground-based, was done, yet with a shorter data series, from 2005 to 2017, considering clear-sky days and data collected around noon time (Figure 2). The data series was shortened to be used in this analysis because the original data series, from Brewer and from OMI, differ in length. In order to perform

https://doi.org/10.5194/egusphere-2023-1474
Preprint. Discussion started: 22 August 2023


the correlation analysis, it is necessary that both data series consist of the same length of values. Linear regression between UV index values from OMI and Brewer confirmed a strong correlation with correlation coefficient (r) of 0.95. MABE values indicate that the difference between daily measurements are small, 0,02% and RMSE was 0,30%. It means a positive correlation was found and the datasets do not vary much when compared to each other. The typical pattern identified and good agreement between ground and satellite UV radiation found in this study was also reported by cadet2017comparison for Reunion site, when considering clear-sky conditions. There is an overestimation of satellite-derived UV measurements when compared to ground-based data, reported by many authors. It is attributed to many factors influencing satellite and surface measurements, including aerosol load in the atmosphere, site elevation, and cloud cover at the time of measurement (Antón et al., 2010; Antón et al., 2007; Ialongo et al., 2011; Kazadzis et al., 2009). Although study location is not of high altitude (488 m) and is not influenced by local geography because geomorphology of the site consists in a wade area without great declination. Moreover, the observatory is located is a rural area, reducing the influence great loads of aerosol directly.

### 3.2 Ground measurements of solar UV index climatology

Distribution of UV index, from the year of 2005 to 2017, can be observed in Figure 3. UV index daily mean is distributed along hours of day, in local time, as well as standard deviation and maximum values of UV index along the period. Typical daily behaviour of UV Index is observed, starting low with as the sun rise, reaching its peak around noon, precisely 12:30 minutes, when daily mean of UV index reached 6, and then decreasing along during the afternoon. Monthly mean of UV index of all sky conditions showed a maximum UV index of 12 (extreme) concentrated mostly in January and December, as in Figure 3 plot below on the right, adjusted to better see the seasonal behaviour of UV index during the year. The months that correspond to the beginning of autumn and end of spring of year UV index vary between 10 and 8, which are already very high values. During the remaining months climatological UVI values are lower, being June and July with the lowest level registered, they vary between 2 and 4 (moderate). Daily mean of each season corroborates with monthly mean of all period, during summer and spring seasons (Figure 4) daily mean vary between 9 and 6, while maximum values registered are extreme, including on autumn, when maximum value was around 12. Those means were calculated considering all sky conditions so it has to be considered that even with attenuation by clouds high and very high values are reached mostly of the year. Clear-sky days were analysed separately, as it is seen in Figure 5, the distribution of days with clear-sky conditions (plot on top), daily mean, with standard deviation and maximum values of UV index, plot below on the left and monthly mean on plot below on the right. The distribution of the days with clear-sky conditions achieved extreme values, almost 16 in the scale, those are due to less attenuation of radiation by clouds. UV index daily mean was almost 8, the maximum values of UV index started already around 9h in the morning and reach almost 16 (extreme > 11) at noon time and at least until 17h UV index levels are still high (from 6 to 7). Monthly mean of UV index reached the same 12 in scale of all-sky conditions, but presented to be much higher over a longer period of the year from September to March. Extreme values were measured from November to December, beginning of summer season and continued along the summer in January and February. UV index increases on the beginning of September, almost spring season and on the end of March, beginning of the fall season but still with very high values of UV

https://doi.org/10.5194/egusphere-2023-1474
Preprint. Discussion started: 22 August 2023


index, which vary between 8 and 10. Maximum UV index in summer reaches almost 16 (Figure 5) and the maximum daily mean is 13 (extreme), in contrast during winter, the maximum is 7 and daily mean is almost 4, during summer the insolation is at least three hours longer than winter and the around 10h in the morning UV index levels already reach very high (between 8 and 10) in the scale. A very similar scenario occurs on the mornings of spring but high values are registered at least until 15h in the afternoon while in summer high UV index persist until 17h. Maximum UV index during spring is 14, extreme and the daily mean reaches 10 (very high). During autumn season the maximum UV index is registered as 12, which is consistent with is observable in the monthly mean, it is extreme UV index although the daily mean on that season reaches 7 (high).

This overview shows that mostly of the year maximum UV index levels are extreme, at least 9 months registered maximum levels above 11 on the scale. Looking at the daily mean of each season it varies from moderate in winter, and extreme in summer, whereas mainly of the year with daily means upper than high levels of UV index. That leads to the discussion on the importance of extra care with sun exposure during the most part of the year and not only during summer season. It was reported by weihs2008measurements a great difference between UV measurements on clear-sky and allsky conditions when ground and satellite were compared. Clear-sky conditions resulted in a low difference between them and from partially cloud to overcast the mean bias between ground and satellite were much higher. Aerosols can interfere in UV radiation intensity by reducing it between 10 to 15% due to absorption (Fioletov et al., 2010; du Preez et al., 2021), especially urban and high load pollution areas, although the site of study is in the rural area with relatively clean background atmosphere and the aerosol interference was not accounted in this study. The frequency of UV index based on the number of days with observations of UV index along the period of the years 2005 to 2017 is represented in Figure 6. Number of days with UV index measures with all-sky conditions is 2460 days and from those, 423 days were selected as days with clear-sky conditions, it was selected the maximum UV index registered in each day and then calculated the percentage of days with each UV index level reached. This result is important because it shows clearly the occurrence of extreme and high levels of UV index, based on the UV index scale, along the year and including in all-sky conditions, when it is expected to have lower levels. Low UV index (lower than 2) was more frequent during winter season and specially in cloud cover conditions, while in clear-sky conditions in the same season, the maximum UV index per day observed, reached moderate on the scale (between 3 and 5). Clear-sky conditions tend to have higher UV index due to less attenuation effects by clouds than all-sky days. Extreme UV index was predominant during the months of summer, from December to January in both all-sky and clear-sky conditions. September with all-sky conditions showed 20% of very high UV index, differently of the same month in clear-sky conditions. Although cloud reflection tends to attenuate UV radiation, depending on the density, type and cloud configuration the reflectivity can cause an increase of UV radiation on the surface, as it was described by (Tiba, 2017) the enhancement in UV radiation lasts for a few minutes, around 6 minutes and can be more significant that global irradiance can be higher than in a day with clear sky condition. So that, very high levels of UV index in all sky conditions in September could be attributed to increase of UV radiation due to cloud reflection. It calls the attention to the month October in both sky conditions, when very high UV index (from 8 to 10) were above 40% in all-sky and above 60% in clear-sky, while the climatological mean for October is 7.96, between 2005 and 2017. Extreme UV index levels were also observed on this month being almost 40% of maximum UV index per day extreme on

https://doi.org/10.5194/egusphere-2023-1474
Preprint. Discussion started: 22 August 2023


clear sky days. It might be linked to low ozone on the region at this time of year due to secondary effects of ozone hole. First observations of those events were reported by Kirchhoff (1996), and Bittencourt (2018) did a thorough study on event occurred in October 2016, showing a great decrease of 23% in ozone total column caused by air mass poor in ozone from brought to the region of study. That goes along with extreme measures of UV index collected.

### 3.3 Interannual variability of UV radiation

The data used in the study of interannual variabilities and periodicity of UV index in the south of Brazil was done with the reconstruction of Brewer ground-based data together with satellite observations from OMI. It was used UV index of clear-sky conditions from Brewer, the missing data was completed with UV index from OMI and the eventual gaps found in data set Brewer-OMI were filled with mean values of the most proximate dates on the data set. This study was developed with data from 2005 to 2017, the annual distribution of UV index is seen in Figure 8. Anomaly of Brewer-OMI data series can be seen in Figure 9a, it was calculated in order to remove the strong annual periodicity and to be able to see other influences in wavelet analysis of anomaly (Figure 9b). Influence of QBO is indicated in the region between 16-32 months of the wavelet power spectrum and also in Figure 9c, the Global wavelet spectrum. QBO can cause great influence in UV-radiation through the interference in stratospheric ozone, as there is evidence of the increase in UV irradiance when in east phase of QBO and the opposite, decrease in UV irradiance when west phase of QBO (Troshichev and Gabis, 1998). In second half of QBO phase there is an easterly shear that causes an upward secondary circulation, resulting in a decrease in ozone, as described by Herman (2000) those dynamic effects of QBO implies a 5-year periodicity variation of UV-B, even greater variability than the one caused by cloud cover. Influence of El-Niño Southern Oscillation depend on the phase. La Niña provokes drought on the region of study and El Niño results in an intensification of rainfall, which is more likely by the result showed in wavelet analysis, in the region corresponding to 64 months. Besides increase of cloud cover during periods of rainfall, ENSO also interferes in Brewer Dobson circulation, in El Niño phase there is an enhancement in upwelling of the Brewer-Dobson circulation in tropical stratosphere depleting ozone on tropical region. The opposite is observed in La Niña phase (Manatsa and Mukwada, 2015). Solar cycle is evident in wavelet analysis in region of 128 months, changes in UV irradiance can be driven even by short-term oscillations in solar activity such as solar protons events and solar flares, responsible for increase in UV radiation (Troshichev and Gabis, 1998).

### 3.4 UV radiation during the events of secondary effects of Antarctic ozone hole

The events were selected based on some criteria, first the availability of ground data of UV index and UV-B, considering there are many gaps in the UV radiation data series, second, the sky condition during the days of events. It is very complex to determine the exactly amount of UV radiation incident on the surface when in presence of clouds, as well as to precise the time when UV radiation is more or less intense with a cloudy sky. Since in cloudy days the resulting effects of variation of ozone total column on UV radiation could be masked and lead us to erroneous results (Guarnieri et al., 2004), then it was considered in the analysis of the events of secondary effects of Antarctic ozone hole, only days with clear-sky conditions, so

https://doi.org/10.5194/egusphere-2023-1474
Preprint. Discussion started: 22 August 2023


considering the persistence of ozone poor air masses over the region of study for a couple of days until ozone total column is re-established (BITTENCOURT et al., 2018) in case of first day of event occurred in cloudy sky condition, it was defined one clear sky-day during the days of events to be looked closely. Ozone total column of this day was compared with UV index (Table 4.1) and UV-B non-weighted (Table 4.2), separately. The daily values were compared with monthly climatological average, used as a reference here to evaluate how much depletion of ozone 63 and increase of UV radiation there were. So that, the percentage of increase of UV index and UV-B non-weighted was calculated as well as the percentage decrease of ozone total column. Among all events studied in this research regarding to UV index and ozone total column analysis (Table 4.1), 60% resulted in 4% UV index increase for each 1% ozone total column depletion, with the exception of the one on October 14, 2012 which resulted in 3.65% increase in UV index, even though a very high increase. Two events showed increase of UV index higher than 4% while only 1 event had an increase of 1% of UV index for a 1% depletion of ozone total column. Ozone total column ranged between 220 and 260 DU around the days of events. It was observed that ozone total column tends to decrease rapidly on the events, furthermore it takes a few days to be re-established, tending to increase slowly and gradually. It was also observed it takes a mean of two days to ozone total column start to be re-established and almost 5 days to ozone total column reach the monthly climatological average after the first day of event. There were two events accounted in 2005, the one in September shows an increase of UV index of almost 1% more than the event in October. That could be related to different climatological mean of each month that varies from 6.01 in September to 7.96 in October, even though the ozone total column decrease in the event of September was 2.8% higher than in October. Only one event was accounted in 2007, it occurred in October and despite of the 8% ozone total column depletion there was an increase in UV index of 8%, in regard to the climatological mean. There was the slightly increase of 1% of UV index for each 1% ozone total column decrease. The two events occurred in 2008 are similar to the ones from 2005 except they appeared to be more intense, specially the one in September, as in terms of decrease in ozone total column as in terms of the increase of UV index. Even though the climatological mean is lower in September, the ozone depletion was very significant, leading to almost 59% UV index increase. The event on October, 2008 ozone depletion was only 2,6% less than the previous event however resulted in 81% increase in UV index, leading to extreme UV index and resulting in the alarming 6,7% UV index increase for each 1% ozone depletion. In 2012 there were three events included here. Two events in September with a very similar behaviour, with almost 10% ozone depletion but with the significant increase of 40% of UV index in the first and the second only 6,6% ozone decrease which resulted in 34% UV index increase, both of them UV index reached very high, according to the scale. One event in October, 2012 showed different behaviour, UV index reached extreme and ozone depletion was more significant than the previous ones, 13% lower than the climatological mean.

Two events were selected from 2016, one event in August resulted in more than 50% increase in UV index due to a 12,8% ozone content depletion. Meaning a 4,3% increase in UV index for each 1% ozone decrease. Although the event was significant in terms of increase of UV radiation, UV index reached high in the scale, probably due to the winter season, when UV radiation is naturally lower. The second event from 2016 was considered a major event of ozone depletion and as a consequence UV radiation increase. Thus, this event was chosen as a study case in the following session. UV-B non-weighted is a measure of

https://doi.org/10.5194/egusphere-2023-1474
Preprint. Discussion started: 22 August 2023


UV-B without any filters such as biological filters of DNA, erythema or UV index, so that it is important to be compared with ozone total column. Differently from UV index analysis, the analysis of UV-B non-weighted, in Table 4.2, showed a very significant increase with ozone depletion, which is expected since it is a direct measured. The exact same ten events from previous analysis with UV index were studied using UV-B non-weighted measures. The events in 2005 were very similar, with greater increase of UV index in the event of September but almost extreme UV index reached in the event of October. The event in 2007 had minor effects on UV index compared with all the other events, resulting in only 9.1% UV index increase for each 1% ozone depletion. UV index that day was slightly above climatological mean. There were two events in 2008, being the one occurred in October with the major increase of UV index. It was 224% higher than the climatological mean, resulting in UV-B non-weighted of 2480 W/m2. All three events occurred in 2012 were very similar regarding to the increase of UV-B non-weighted. A curious detail in the event on September 22 when the decrease in ozone total column was of 6% in relation to the climatological mean and the increase of UV-B non-weighted was 15% for each 1% ozone depletion, while the other event, in September 14 the drop was 9%, leading to 11% UV-B increase for each 1% ozone depletion. This could be due to the second event is in the end of September is closer to October when the UV radiation naturally intensifies, due to the change of seasons. In addition, the event in October 14, showed same behaviour of the first event in September, probably due to the higher climatological mean. The three events had an increase of more than 100% in UV-B non-weighted. In 2016 there was one event in August, with more than 150% increase in UV-B non-weighted, it resulted in 13% increase in UV-B for each 1% ozone depletion. The increase of UV-B non-weighted in the event of October 21, 2016 was more than 200% with 19% ozone content depletion. Generally, the daily values of UV-B on the days of events selected are at least 100% higher than the climatological monthly mean, with only one exception. Daily values reached more than 200% increase in two events, October 27, 2008 and August 25, 2016. The event on October, 2007 showed the lowest increase of UV-B, resulted in 77% of increase in relation with the climatological mean. Overall, the mean of UV-B non-weighted increase with 1% decrease of ozone total column was 13%.

A study developed by Guarnieri et al. (2004) on the same location of the present study, showed a major influence of ozone variation on UV-B radiation, suggesting 94% of UV radiation variability would have been caused by ozone changes when analysing clear sky days. Resulting in a UV-B enhancement ranging from 0.87% to 1.43%, depending on the solar zenith angle, for each 1% of ozone depletion. Regarding to ozone total column, a usual content on the region of study consists in approximate 280 DU which is also observed on the months studied, usually far from the day of event. Concentrations that are characteristic of the ozone hole are values below 220 DU, on the Antarctic region (Hofmann et al., 1997). du Preez et al. (2019) estimated in his study in South Africa, in clear-sky conditions 1% decrease of ozone total column would result in 0.59% increase of UVB radiation on the surface, using clear-sky determination method of radiation amplification factor. In the same study, specifically, in events of ozone depletion and with clear-sky conditions, UV radiation increases from 6 to 45% with variations in ozone total column. Reported by Raptis et al. (2021) as a rare low ozone event, in the region of Athens, Greece, caused the increase of approximately 30% in the UV radiation, when the decrease in ozone total column was of 15% in relation to the climatological monthly mean. Generally, the decrease in ozone total column with the arrival of polar masses appear to

https://doi.org/10.5194/egusphere-2023-1474
Preprint. Discussion started: 22 August 2023


be more intense in the year of 2008 and from 2012 until 2016, despite the positive scenario describing the healing of Antarctic ozone hole by Solomon et al. (2016). The response of UV index to lower ozone content, is in similar proportion, with few exceptions. The events on September appear to be have major ozone decrease than the events in October, probably because it is the first period of weakening of Polar vortex, releasing filaments with lowest ozone content. With exception of event of October, 2016, probably due to the time of year when radiation already tends to be higher. Through this research it was filled a gap regarding updates in UV radiation and events of secondary effects of Antarctic ozone hole specific on the south region Brazil. It is suggested the investigation of more events in future studies. Aside of that, different mid-latitude regions could be studied regarding UV radiation behaviour during those events, besides south of Brazil. Since aerosol loads can interfere on UV radiation intensity on the surface, those measurements from Brewer spectrophotometer could also be accounted for future studies of UV radiation on the region.

### 3.4.1 Event of secondary effects of Antarctic ozone hole on October, 2016

The study case is about one of the most significant events of secondary effects of Antarctic ozone hole, occurred between 2005 and 2016 and considered one of the most intense events in the last 25 years. This event was persistent starting from October 20, 2016 68 and it is detailed discussed in this section. Ozone total column measured with the Brewer spectrophotometer used in this study, was 225.5 Dobson Units on October 20, there was a 23% decrease in relation to the climatological mean for October (from 1992 to 2016), a very critical reduction as reported by Bittencourt et al. (2018). The following day, October 21, the poor-ozone air mass was still on the region but showed a slightly recover, ozone total column was 19% below the climatological mean. With the observation of extreme reduction in ozone total column in relation to the climatological mean, it was identified the event. Then, the potential vorticity analysis confirmed the origin of air mass is from Antarctic region. It acts as a dynamic tracer for those large air-masses and is correlated with the transport of chemical constituent traces, as ozone. Figure 4.16 shows the maps of potential vorticity in the level of potential temperature of 700 Kelvin. It is observed its progress towards the study region. The images show the increase in Absolute potential vorticity, indicating the reduction in ozone content.

Images of October 19 to 21, 2016 from OMI satellite (Figure (4.17) in a global and South Pole perspectives show AOH over the region and its influence in mid-latitude regions. According to these images, poor-ozone air masses that reached the region of study range from 250 and 200 Dobson Units, while in South Pole region ozone content is even lower. The study of the backward trajectories of ozone-poor air masses in different heights are shown in Figure (4.18). It is an image from HYSPLIT, a model from NOAA that shows the air mass dispersion and it is used to trace air mass trajectories. It contains the path followed by ozone-poor air masses in October 20 (a) and 21 (b), 2016, at 28, 24 and 20 km height and it is seen it reached the study region (BRESCIANI et al., 2018). The day selected to have UV radiation analysed was October 21 due to the clear-sky condition, confirmed using the method previously described of Gaussian analysis. Maximum UV index per day between October 10 and 31, 2016 is shown in Figure 4.19, as well as daily ozone total column. An image via GOES 13 Satellite of thermal infrared channel shows the absence of clouds at this day (Figure 4.20). UV index was 10 (very high in UV index

https://doi.org/10.5194/egusphere-2023-1474
Preprint. Discussion started: 22 August 2023


scale), on October 20, however, on the day after, October 21, UV index from Brewer reached 15 while the climatological monthly mean is almost 8 in UV index scale. It resulted in 88.53% increase in UV index in relation to the climatological mean of the month, while the anomaly of ozone total column was -19.77% in relation to the climatological mean of the month. The following days, UV index levels slowly diminished as ozone total column gradually recovered. This was considered the most significant day in UV radiation increase, each 1% reduction in ozone total column there was an increase of 4.47% in UV index. Apparently, air mass poor in ozone was persistent for five days. It was suggested by Bittencourt et al. (2018) the air transport between stratosphere and troposphere were intensified by the presence of subtropical jet combined with positive omega values at 500 hPa, which might be one of the responsible factors for such extreme event. The identification of numerous events of secondary effects of Antarctic ozone hole enabled to learn UV radiation response on the south of Brazil. It was confirmed the fast response of UV radiation in reduction of ozone total column and the alarming levels reached by UV index during the events. It is crucial information for public health because once the population is aware about the existence and how these events impact surface solar UV, precautions can be taken. Besides human health, the increase in UV radiation during this period also affects fauna and flora, another concern to be considered when finding ways to mitigate the effects of the events of secondary effects of AOH. Besides health issues related to excess exposure to UV radiation, sunlight is essential to human life in many ways. The synthesis of vitamin D only happens with skin exposure to the sun and it is known that this hormone plays a key role in immune system of the body. Aranow (2011) said "Vitamin D can modulate the innate and adaptive immune responses. Deficiency in vitamin D is associated with increase autoimmunity and an increased susceptibility to infection". Vitamin D is directly linked to the promotion of bone health because it enhances calcium absorption besides the mineralization of the collagen matrix in bone. In such manner, population is provided with a great amount of solar radiation enabling the syntheses of vitamin D through sunbath. Results founded in this study are extremely important and could be used for a public campaign with accessible information about this matter to raise public awareness about occurrence period, region of impact and how it affects human and animal health.

## 4 Conclusions

Ground and satellite resulted in a good agreement between them without strong scatter in their correlation. Periodicity of UV index showed a clear seasonal variation on the study region. Besides, that cloud cover causes great impact on UV radiation intensity on the surface, especially because the region of study is characterized by active rainfall regime along the year. UV index tends to be 44% higher when in clear-sky conditions during summer and spring periods and extreme values are reached along summer season, yet depending on the cloud formation an increase in UV radiation can happen. Overall UV index shows a typical behaviour of the radiation during the day, reaching its peak around noon time and during the year, making the seasons of the year in the south of Brazil well delimited. One must be attentive to sun exposure because UV index can reach high and extreme levels almost all year. As it was observed, the maximum UV index per season, safety precautions should be taken even in winter, when the UV index levels still reach extreme levels. Wavelet analysis showed that variability of UV radiation could results from QBO, ENSO and solar cycle forcing, due to their contribution to stratospheric ozone variability.

https://doi.org/10.5194/egusphere-2023-1474
Preprint. Discussion started: 22 August 2023


The events of secondary effects of Antarctic ozone hole selected to be analyzed range from 2005 to 2016. Five of the ten events studied happened in October, mid of spring season, during the weakening of Antarctic polar vortex, other four events in September and one in August. Which reflexes in occurrence of extreme values nearly 40% of October months in days of clear-sky condition. It was found that for every 1% reduction in ozone total column on the region, during the passage of those air masses poor in ozone, there were 4% of increase in UV index in the region, so it is evident the secondary effects of Antarctic ozone hole over the study region. Even though cloudy days can mask the effects of ozone depletion on surface UV, it is important to consider that the poor-ozone air mass can be persistent for a few days on the region. This study only considered one day of event, being it with a clear-sky condition, a few more days with clear sky condition can happen, prolonging the effects of the event on surface UV, so that it is important to consider extending the study for more clear-sky days instead of considering only one day of each event. Moreover, it is suggested from the present study that months when there are secondary effects of Antarctic ozone hole (spring time) should be further investigated. It is also recommended to study the influence of aerosols on UV index variations, especially during the Amazon fire season which, through atmospheric transport processes, may extend and concern southern Brazil (Bencherif et al., 2020).

With the results founded, it is possible to raise awareness on the population on behalf of occurrence of those events, the proportion they might take and all precautions people could have in order to avoid excess exposure to UV radiation, especially during a period of year people are not expecting to have such extreme values of UV index, differently from summer season when there is already expectations.

Author contributions. BC, DP, HB, TP, LP, GB and NT designed the methodology and BC, JM, DP, LP performed the analysis. BC, DP, HB, TP, LP, GB and NT contributed to the discussion of the results. BC, DP, LP and GB prepared the manuscript with contributions from all co-authors.

Competing interests. The authors declare that they have no conflict of interest.

Acknowledgements. This work is part of the MESO Project "Modelling and forecasting the secondary effects of the Antarctic ozone hole", registered under no. 8887.130199/2017-00. The authors would like to thank the CAPES (Coordination of Improvement of Higher Education Personnel) and COFECUB (French Committee for the Evaluation of University Cooperation with Brazil) program responsible for promoting this research.

https://doi.org/10.5194/egusphere-2023-1474
Preprint. Discussion started: 22 August 2023


## References

Al-Aidaroos, A. M., El-Sherbiny, M. M., Satheesh, S., Mantha, G., Agustïs, S., and Carreja, B.: High mortality of Red Sea zooplankton under ambient solar radiation, Plos One, 9, https://doi.org/10.1371/journal.pone.0108778, 2014.

Antón, M., Cachorro, V., Vilaplana, J., Toledano, C., Krotkov, N., and Arola, A.: Comparison of UV irradiances from Aura/Ozone Monitoring Instrument (OMI) with Brewer measurements at El Arenosillo (Spain)–part 1: Analysis of parameter influence, Atmos. Chem. Phys., 10, 5979–5989, https://doi.org/10.5194/acp-10-5979-2010, 2010.

Antón, M., Cachorro, V., Vilaplana, J., Krotkov, N., Serrano, A., and Toledano, C.: Total ozone mapping spectrometer retrievals of noon erythemal-CIE ultraviolet irradiance compared with Brewer ground-based measurements at El Arenosillo (southwestern Spain), J. Geophy. Res-Atmos., 112, https://doi.org/10.1029/2006JD007254, 2007.

Aranow, C.: Vitamin d and the immune system. J. Investig. Med., 59, 6, 881–886, https://doi.org/10.2310/JIM.0b013e31821b8755, 2011.

Bittencourt, G. D.: Influência da dinâmica atmosférica durante eventos de efeito secundário do buraco de ozônio antártico sobre o sul do brasil. M.S. Federal University of Santa Maria, 2018.

Bencherif, H., Bègue, N., Kirsch, P. D., du Preez D. J., Cadet J. M., and da Silva Lopes F. J.: Investigating the Long-Range Transport of Aerosol Plumes Following the Amazon Fires (August 2019): A Multi-Instrumental Approach from Ground-Based and Satellite Observations, Remote Sens., *12*, 3846. https://doi.org/10.3390/rs12223846, 2020.

Bittencourt, G. D., Bresciani, C., Kirsch Pinheiro, D., Bageston, J. V., Schuch, N. J., Bencherif, H., Leme, N. P., and Vaz Peres, L.: A major event of Antarctic ozone hole influence in southern Brazil in October 2016: an analysis of tropospheric and stratospheric dynamics, Ann. Geophys., 36, 415–424, https://doi.org/10.5194/angeo-36-415-2018, 2018.

Cadet, J., Sage, E., Douki, T.: Ultraviolet radiation-mediated damage to cellular DNA. Mutat. Res., 571, 3–17, https://doi.org/10.1016/j.mrfmmm.2004.09.012, 2005.

Cadet, J. M. et al.: Comparison of ground-based and satellite-derived solar UV index levels at six south African sites, Int. J. Environ. Res. Public Health, 14, 1384, https://doi.org/10.3390/ijerph14111384, 2017.

https://doi.org/10.5194/egusphere-2023-1474
Preprint. Discussion started: 22 August 2023


Cavalcante, F., Ferreira, N., Dias, M., and Justi, M.: Tempo e Clima no Brasil, São Paulo: Oficina de Textos, v. 1. ISBN 978-85-86238-92-5; 2009.

Copernicus Publications: https://www.copernicus.eu/en/news/news/observer-evolution-ozone-hole-1979-2021, last access: 21 June 2023.

CPTEC, C. de Previsão de tempo e estudos climáticos Instituto Nacional de P. E. Thermal infrared channel. 2017. Available in: <http://satelite.cptec.inpe..br/home/index.jsp>.

Daubechies, I. Ten Lectures on Wavelets. Conference Series in Applied Mathematics. SIAM, NSF, Philadelphia, PA, EUA,1992.

de Paula, M. C. and Pires L. C. M.: Doses of erythemal ultraviolet radiation observed in Brazil. Int. J. Dermatol., 52, 966–973, https://doi.org/10.1111/j.1365-4632.2012.05834.x, 2013.

Douglass, A. R., Newman, P. A., and Solomon, S. The Antarctic ozone hole: An update, Phys. Today, 67, 42–48, https://doi.org/10.1063/PT.3.2449, 2014

du Preez, D. J., Ajtić, J. V., Bencherif, H., Bègue, N., Cadet, J.-M., and Wright, C. Y.: Spring and summer time ozone and solar ultraviolet radiation variations over Cape Point, South Africa, Ann. Geophys., 37, 129–141, https://doi.org/10.5194/angeo-37-129-2019, 2019.

du Preez, D. J., Bencherif, H., Portafaix, T., Lamy, K., and Wright, C. Y.: Solar Ultraviolet Radiation in Pretoria and Its Relations to Aerosols and Tropospheric Ozone during the Biomass Burning Season, Atmosphere, 12, 132, https://doi.org/10.3390/atmos12020132, 2021.

Elías, A. and Zossi, M.: A search for an association between the equatorial stratospheric QBO and solar UV irradiance. Geophys. Res. Lett., 30, https://doi.org/10.1029/2003GL017771, 2003.

Engelsen, O.: The relationship between ultraviolet radiation exposure and vitamin D status, Nutrients, 2, 482– 495, https://doi.org/10.3390/nu2050482, 2010.

EPA - Environmental Protection Agency: https://www.epa.gov/sunsafety/uv-index-scale-0, last access: 31 July, 2019.

https://doi.org/10.5194/egusphere-2023-1474
Preprint. Discussion started: 22 August 2023


Fioletov, V., Kerr, J. B., and Fergusson, A.: The UV index: definition, distribution and factors affecting it, Can. J. Public Health, 101, I5–I9, https://doi.org/10.1007/BF03405303, 2010.

Flury, T., Wu, D. L., and Read, W. G.: Variability in the speed of the Brewer–Dobson circulation as observed by Aura/MLS, Atmos. Chem. Phys., 13, 4563–4575, https://doi.org/10.5194/acp-13-4563-2013, 2013.

Foyo-Moreno, I., Alados, I., Olmo, F., Alados-Arboledas, L.: The influence of cloudiness on UV global irradiance (295–385 nm), Agr. Forest. Meteorol., 120, 101–111, https://doi.org/10.1016/j.agrformet.2003.08.023, 2003.

García-Huidobro, M. R. et al.: Seawater-temperature and UV-radiation interaction modifies oxygen consumption, digestive process and growth of an intertidal fish. Mar. Environ. Res., 129, 408–412, https://doi.org/10.1016/j.marenvres.2017.06.013, 2017.

Giovanni Platform, NASA Earth Data, Available online: http:/giovanni.gsf.nasa.gov/giovanni/, last access 8 November 2017.

Grant, R. H., Heisler, G. M.: Estimation of ultraviolet-B irradiance under variable cloud conditions, J. Appl. Meteorol., 39, 904–916, https://doi.org/10.1175/1520-0450(2000)039<0904:EOUBIU>2.0.CO;2, 2000.

Guarnieri, R. A. et al.: Ozone and UV-B radiation anticorrelations at fixed solar zenith angles in southern brazil. Geofís. Int., 43, 17–22, https://doi.org/10.22201/igeof.00167169p.2004.43.1.209, 2002.

Herman, J., Piacentini, R., Ziemke, J., Celarier E, Larko D.: Interannual variability of ozone and UV-B ultraviolet exposure. J. Geophys. Res., 105, 29189–29193, 2000JD900524. 0148-0227/00/2000JD900524509.00, 2000.

Hofmann, D. et al.: Ten years of ozonesonde measurements at the south pole: Implications for recovery of springtime Antarctic ozone, J. Geophys. Res., 102, D7, 8931–8943, 96JD03749. 0148-0227/97/96JD-03749509.00, 1997.

Holick, M. F.: Sunlight, UV-radiation, vitamin D and skin cancer: how much sunlight do we need? Sunlight, vitamin D and skin cancer, Adv. Exp. Med. Biol., 624, 1–15, https://doi.org/10.1007/978-0-387-77574-6_1, 2008.

Hosking, B. J., Mcintyre, M. E., and Robertson, A. W.: On the use and significance of isentropic potential vorticity maps, Q. J. R. Meteor. Soc., 111, 877–946, https://doi.org/10.1002/qj.49711147002, 1985.

Ialongo, I., Casale, G., and Siani, A.: Comparison of total ozone and erythemal UV data from OMI with ground-based measurements at Rome station, Atmos. Chem. Phys., 8, 3283–3289, https://doi.org/10.5194/acp-8-3283-2008, 2008.

https://doi.org/10.5194/egusphere-2023-1474
Preprint. Discussion started: 22 August 2023


Johnson, B. J., Cullis, P., Booth, J., Petropavlovskikh, I., McConville, G., Hassler, B., Morris, G. A., Sterling, C., and Oltmans, S.: South Pole Station ozonesondes: variability and trends in the springtime Antarctic ozone hole 1986–2021 Atmos. Chem. Phys., 23, 3133–3146, https://doi.org/10.5194/acp-23-3133-2023, 2003.

Kazadzis, S., Bais, A., Arola, A., Krotkov, N., Kouremeti, N., and Meleti, C.: Ozone Monitoring Instrument spectral UV irradiance products: comparison with ground based measurements at an urban environment, Atmos. Chem. Phys., 9, 585–594, https://doi.org/10.5194/acp-9-585-2009, 2009.

Kirchhoff, V. et al.: Evidence for an ozone hole perturbation at 30 south. Atmospheric Environment, Elsevier, 30, 9, 1481–1488, 1996.

Lamy, K., Ranaivombola, M., Bencherif, H., Portafaix, T., Toihir, M. A., Lakkala, K., Arola, A., Kujanpää, J., Pitkänen, M. R. A. and Cadet, J. M.: Monitoring solar radiation UV exposure in the Comoros, Int. J. Environ. Res. Public Health, 18, 10475; https://doi.org/10.3390/ijerph181910475, 2021.

Liou, K. N.: An introduction to atmospheric radiation, vol. 84. Elsevier; ISBN: 9780124514515, 2002.

Luiz, E. W., Martins, F. R., Costa, R. S., Goncalves, A. R., de Souza, J. G., de Lima, F. J. L.: Comparação de metodologias para a estimativa da fração de cobertura de nuvens utilizando câmera all-sky e satélite, in: VII Congresso Brasileiro de Energia Solar-CBENS 2018; 2018.

Marchand, M. et al.: Model simulations of the impact of the 2002 Antarctic ozone hole on the midlatitudes, J. Atmos. Sci., 62, 871–884, https://doi.org/10.1175/JAS-3326.1, 2005.

Manatsa, D., Mukwada, G.: A connection from stratospheric ozone to El Niño-Southern Oscillation, Sci. Rep., 7, 5558, https://doi.org/10.1038/s41598-017-05111-8, 2017.

OMI-ERS2/NASA: AURA Validation Data Center, https://avdc. gsfc.nasa.gov/index.php?site=1593048672&id=28, last acces: 23 March 2017.

Ozone Monitoring Instrument (OMI) Team. Data User's Guide; Ozone Monitoring Instrument (OMI): Netherland's Agency for Aerospace Programs (NIVR), Netherland and Finnish Meteorological Institute (FMI): Helsinki, Finland, 2012.

Pfeifer, G. P., Besaratinia, A.: UV wavelength-dependent DNA damage and human non-melanoma and melanoma skin cancer, Photochem. Photobiol. Sci., 11, 90–97, https://doi.org/10.1039/c1pp05144j, 2012.

Peres, L. V.: Monitoramento da coluna total de ozônio e a ocorrência de eventos de influência do buraco de ozônio antártico sobre o sul do Brasil. 2016. Ph.D. Federal University of Santa Maria, 2016.

Raptis, I. P. et al.: The combined effect of ozone and aerosols on erythemal irradiance in an extremely low ozone event during May 2020, Atmosphere, 12, 2, 145, https://doi.org/10.3390/atmos12020145, 2021.

Ries, G., Heller, W., Puchta, H., Sandermann, H., Seidlitz, H. K., and Hohn, B.: Elevated UV-B radiation reduces genome stability in plants, Nature, 406, 98–101, https://doi.org/10.1038/35017595, 2000.

Rolph, G., Stein, A., and Stunder, B.: Real-time environmental applications and display system: Ready, Environ. Modell. Softw., 95, 210–228, https://doi.org/10.1016/j.envsoft.2017.06.0252017, 2017.

Rozema, J., Staaij, J. V., Björn, L. O., Caldwell, M.: UV-B as an environmental factor in plant life: stress and regulation. Trends. Ecol. Evol., 12, 22–28, https://doi.org/10.1016/s0169-5347(96)10062-8, 1997.

Semane, N., Bencherif, H., Morel, B., Hauchecorne, A., and Diab, R. D.: An unusual stratospheric ozone decrease in the Southern Hemisphere subtropics linked to isentropic air-mass transport as observed over Irene (25.5° S, 28.1° E) in mid-May 2002, Atmos. Chem. Phys., 6, 1927–1936, https://doi.org/10.5194/acp-6-1927-2006, 2006.

SCI-TEC, I. I. Brewer Ozone Spectrophotometer Operators Manual MKIII167. 1999. Available in: < https://www.kippzonen.com/Product/50/ Brewer-MkIII-Spectrophotometer#.Yp5Ex6jMKM8>.

Solomon, S. et al.: Emergence of healing in the Antarctic ozone layer, Science, 353, 6296, 269–274, https://doi.org/10.1126/science.aae0061, 2016.

Schafer, J., Saxena, V., Wenny, B., Barnard, W., De Luisi, J.: Observed influence of clouds on ultraviolet-B radiation, Geophys. Res. Lett, 23, 2625–2628, https://doi.org/10.1029/96GL01984, 1996.

Seckmeyer, G., Erb, R., Albold, A.: Transmittance of a cloud is wavelength-dependent in the UV-range, Geophys. Res. Lett., 23, 2753–2755, https://doi.org/10.1029/96GL02614, 1996.

https://doi.org/10.5194/egusphere-2023-1474
Preprint. Discussion started: 22 August 2023


Slater, D., Long, C., Tooman, T.: Total sky imager/whole sky imager cloud fraction comparison, in: Proc. 11th ARM Science Team Meeting, 1-11, 2001.

Tiba, C., and Leal, S. D. S.: Enhancement of UV radiation by cloud effect in NE of Brazil, Int. J. Photoenergy, 2017, 9 https://doi.org/10.1155/2017/8107435, 2017.

Torrence, C.; Compo, G. P.: A practical guide to wavelet analysis. Bulletin of the American Meteorological Society, 79, 61-78, 1998.

Troshichev, O., and Gabis, I.: Variations of solar UV irradiance related to short-term and medium-term changes of solar activity, J. Geophys. Res., 103, 20659–20667, https://doi.org/10.1029/98JA01739, 1998.

Wang, F., Gao, Q., Hu, L., Ge, T., Yu, J., Liu, Y.: Risk of eye damage from the wavelength-dependent biologically effective UVB spectrum irradiances, Plos One, Public Library of Science San Francisco, USA, 7, p. e52259, https://doi.org/10.1371/journal.pone.0052259, 2012.

Wang, F., Ge, T., Gao, Q., Hu, L., Yu, J., and Liu, Y.: The distribution of biologically effective UV spectral irradiances received on a manikin face that cause erythema and skin cancer, J. Photoch. Photobio. B, 140, 205–214, https://doi.org/10.1016/j.jphotobiol.2014.08.004, 2014

WHO, World Health Organization, et al. Ultraviolet Radiation (Environmental Health Criteria 160), Geneva, 1994.

Wuebbles, D.: Ozone Depletion and Related Topics: Ozone Depletion Potentials. In: Encyclopedia of Atmospheric Sciences: Second Edition, Elsevier Inc.; 2015.p. 364–369.

Zhang, J., Tian, W., Xie, F., Li, Y., Wang, F., and Huang, J.: Influence of the El Niño Southern Oscillation on the total ozone column and clear-sky ultraviolet radiation over China, Atmos. Environ., 120, 205–216, https://doi.org/10.1016/j.atmosenv.2015.08.080, 2015.

https://doi.org/10.5194/egusphere-2023-1474
Preprint. Discussion started: 22 August 2023


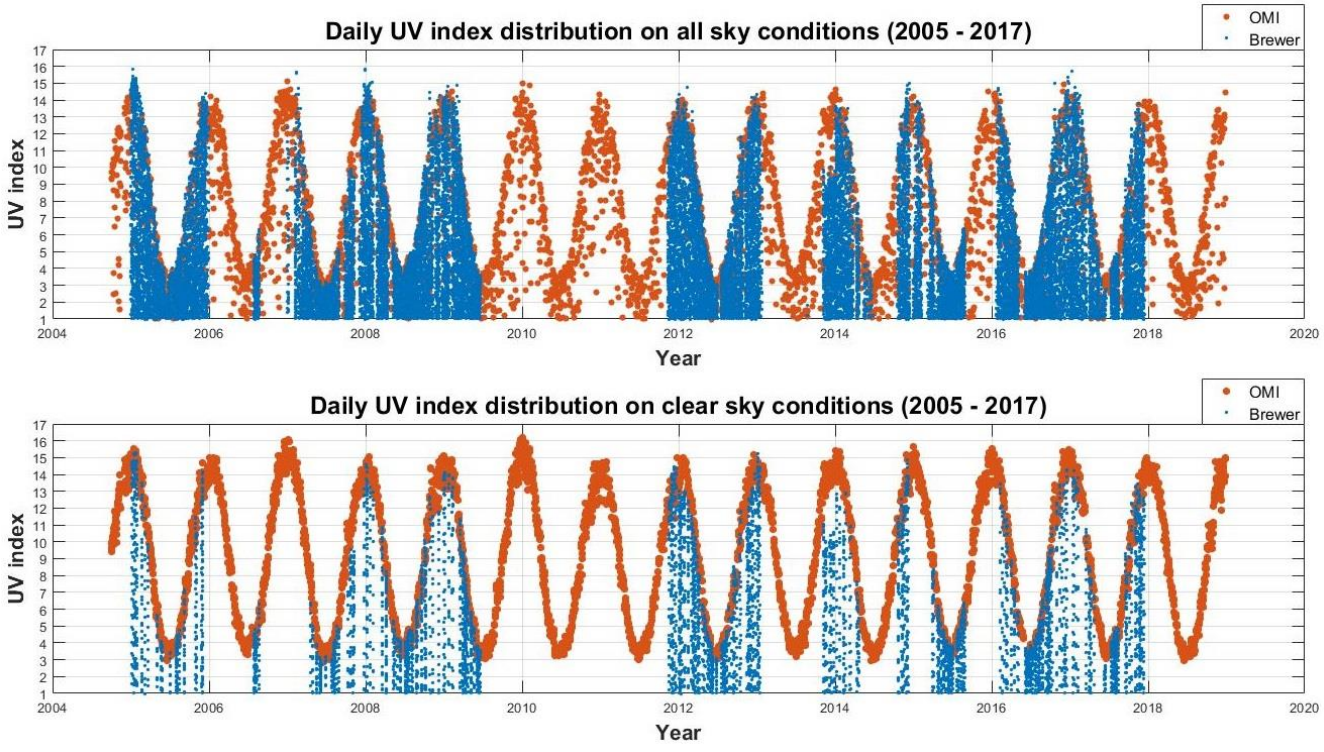


**Figure 1: Comparison of ground and satellite UVI measurements by the Brewer spectrometer (blue dots) and from OMI (orange dots) of all-sky (plot on top) and clear sky conditions (plot below).**

https://doi.org/10.5194/egusphere-2023-1474
Preprint. Discussion started: 22 August 2023


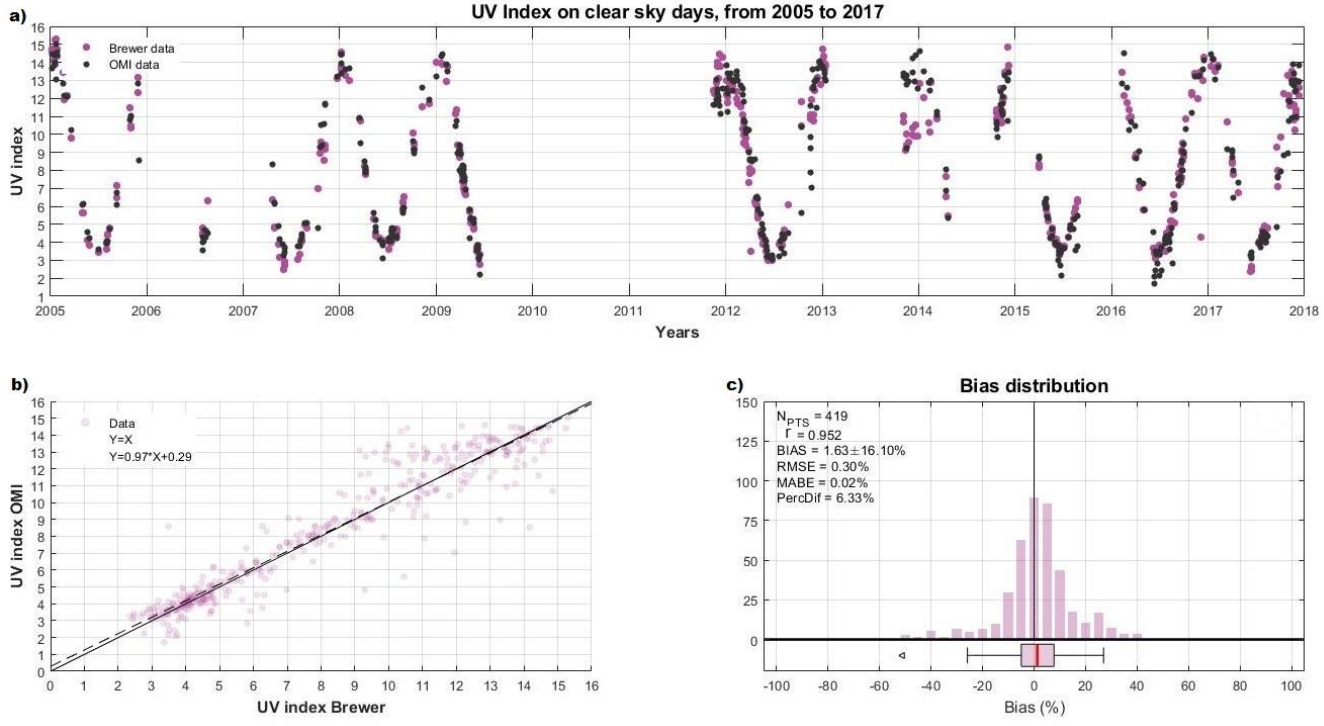


725

**Figure 2: UV index distribution from Brewer and from OMI overlaid, measured around noon time, from 2005 to 2017. Correlation between UV index measured with Brewer and OMI. Bias distribution showing the main difference between UV index from Brewer and OMI.**

https://doi.org/10.5194/egusphere-2023-1474
Preprint. Discussion started: 22 August 2023


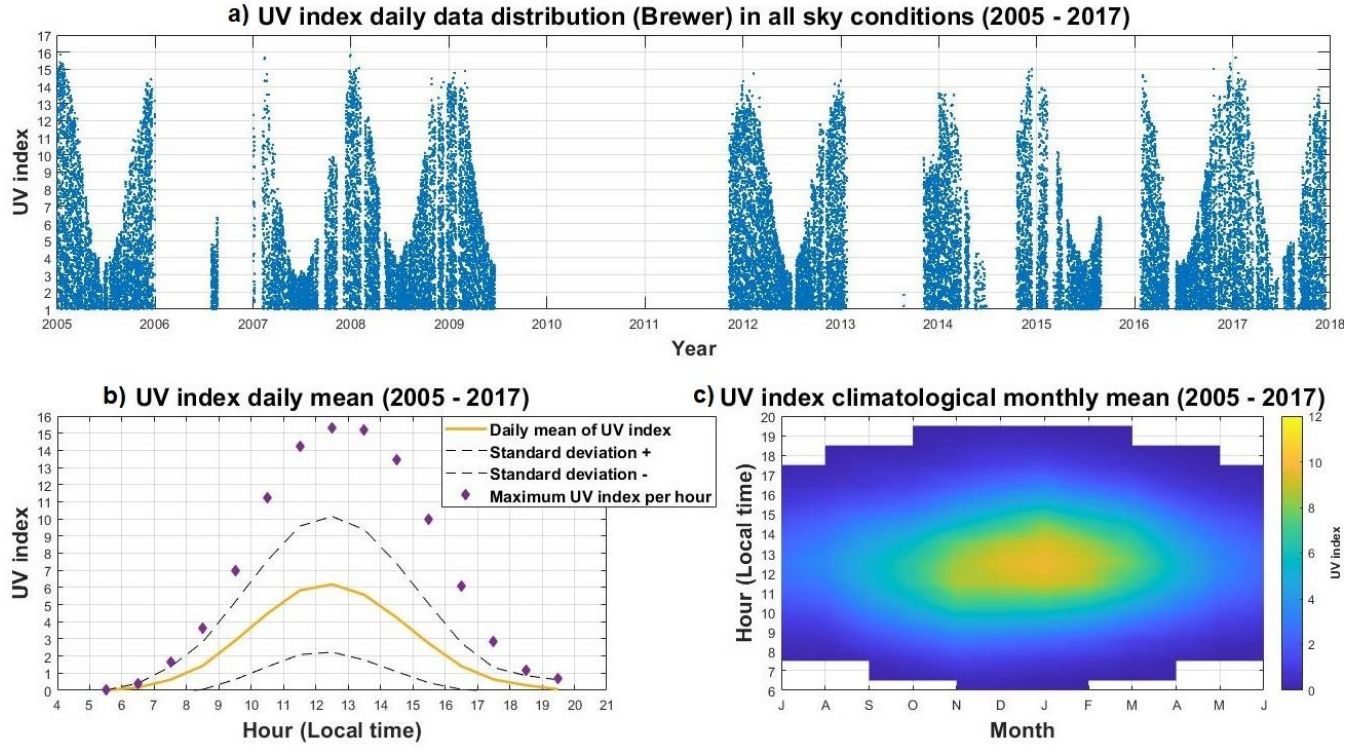


730 **Figure 3: Climatology of UV index on all-sky condition, 2005 to 2017. UV index distribution with all measures of UV index in blue dots, in all-sky conditions, from 2005 to 2017. Daily mean of UV index, in yellow line, shows the mean of all measures in all-sky conditions of UV index during the hours of day, showing the daily behaviour of UV index. Dashed lines are standard deviation and the maximum UV index registered per hour are represented in purple diamonds. Monthly mean of all measures in all-sky conditions are distributed along the months of the year per hour of day, the plot was adapted for better visualization of UV index, represented**
735 **in colour bar.**

https://doi.org/10.5194/egusphere-2023-1474
Preprint. Discussion started: 22 August 2023


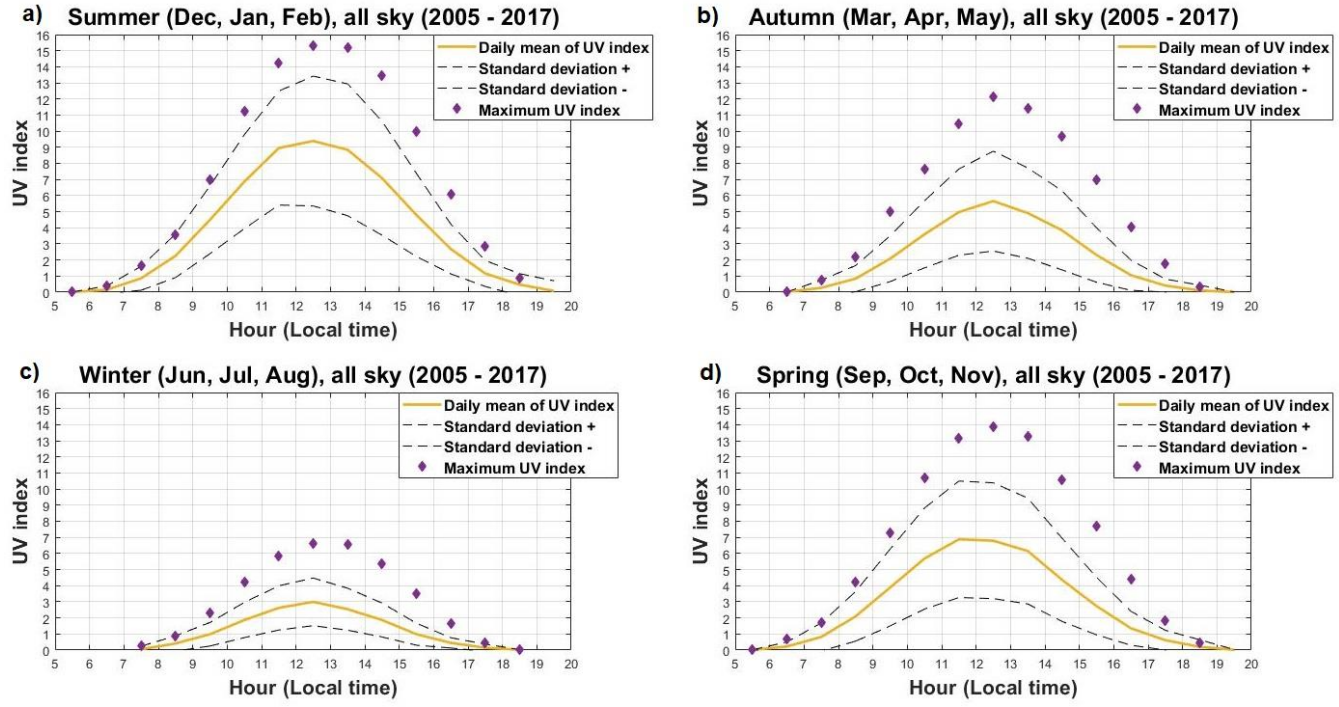


**Figure 4: Daily mean of UV index on all-sky condition (yellow line) per season, summer and autumn plots on top, and winter and spring (plots below). Standard deviation is the dashed line and maximum UV index per hour of day is indicated with purple diamonds. The daily means are from all measures in all-sky conditions from 2005 to 2017.**

https://doi.org/10.5194/egusphere-2023-1474
Preprint. Discussion started: 22 August 2023


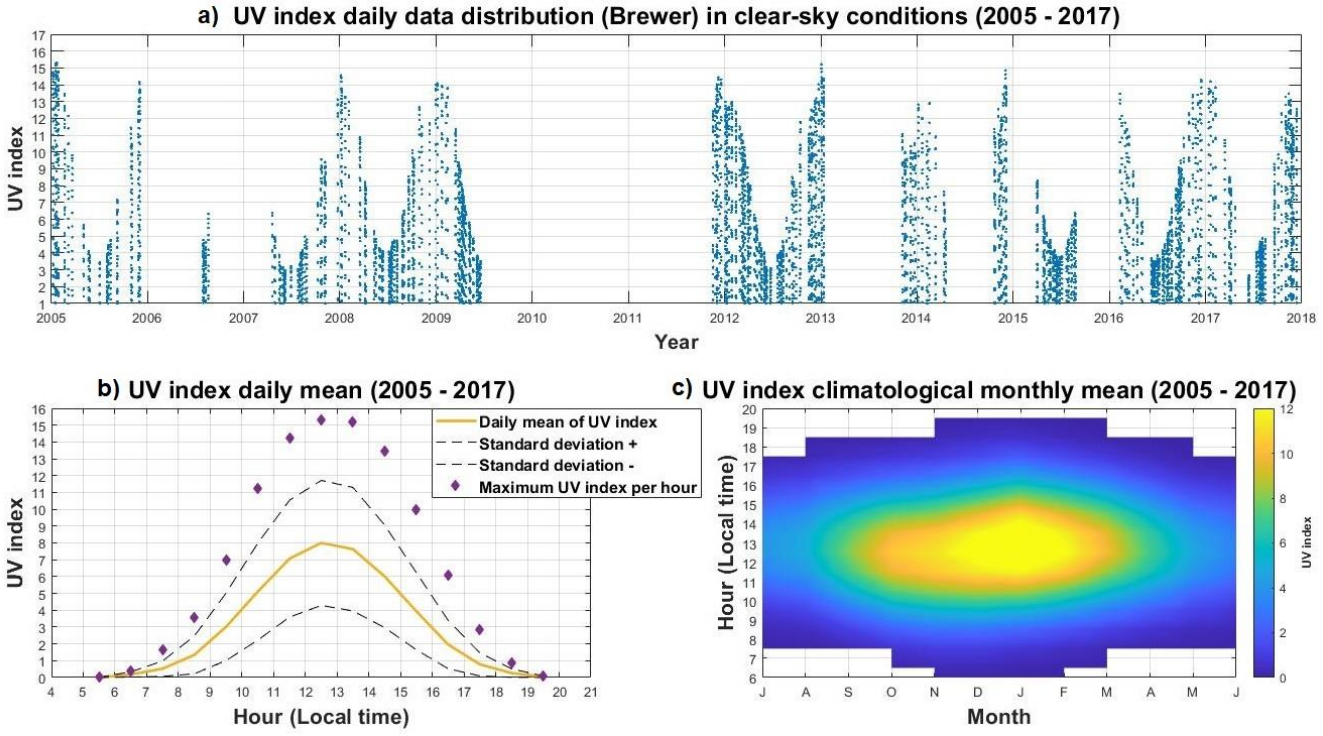


**Figure 5: Climatology of UV index on clear-sky condition, 2005 to 2017. UV index distribution with all measures of UV index in blue dots, in clear-sky conditions, from 2005 to 2017. Daily mean of UV index, in yellow line, shows the mean of all measures in clear-sky conditions of UV index during the hours of day. Standard deviation is represented in dashed lines and the maximum UV index registered per hour are represented in purple diamonds. Monthly mean of all measures in clear-sky conditions are distributed along the months of the year per hour of day, the plot was adapted for better visualization of UV index, represented in colour bar**

https://doi.org/10.5194/egusphere-2023-1474
Preprint. Discussion started: 22 August 2023


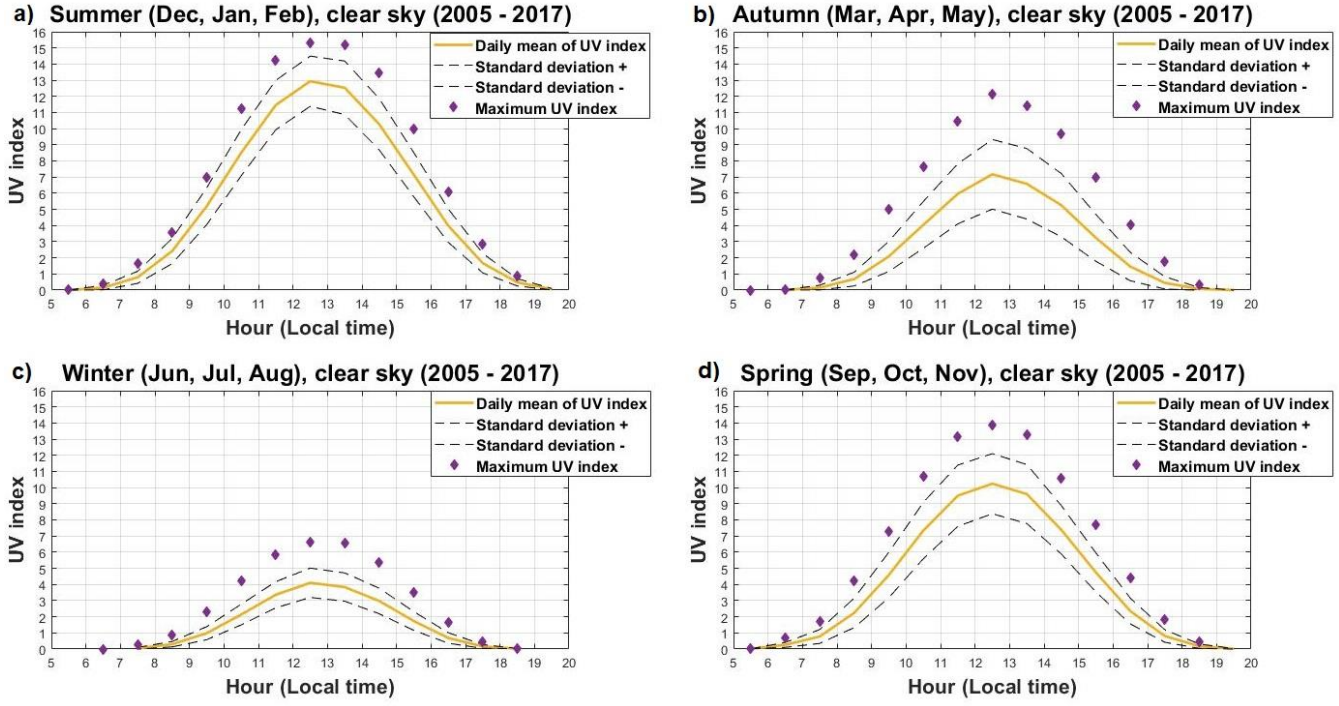


**Figure 6: Daily mean of UV index on all-sky condition (yellow line) per season, summer and autumn plots on top, and winter and spring (plots below). Standard deviation is the dashed line and maximum UV index per hour of day is indicated with purple diamonds. The daily means are from all measures in all-sky conditions from 2005 to 2017.**

https://doi.org/10.5194/egusphere-2023-1474
Preprint. Discussion started: 22 August 2023


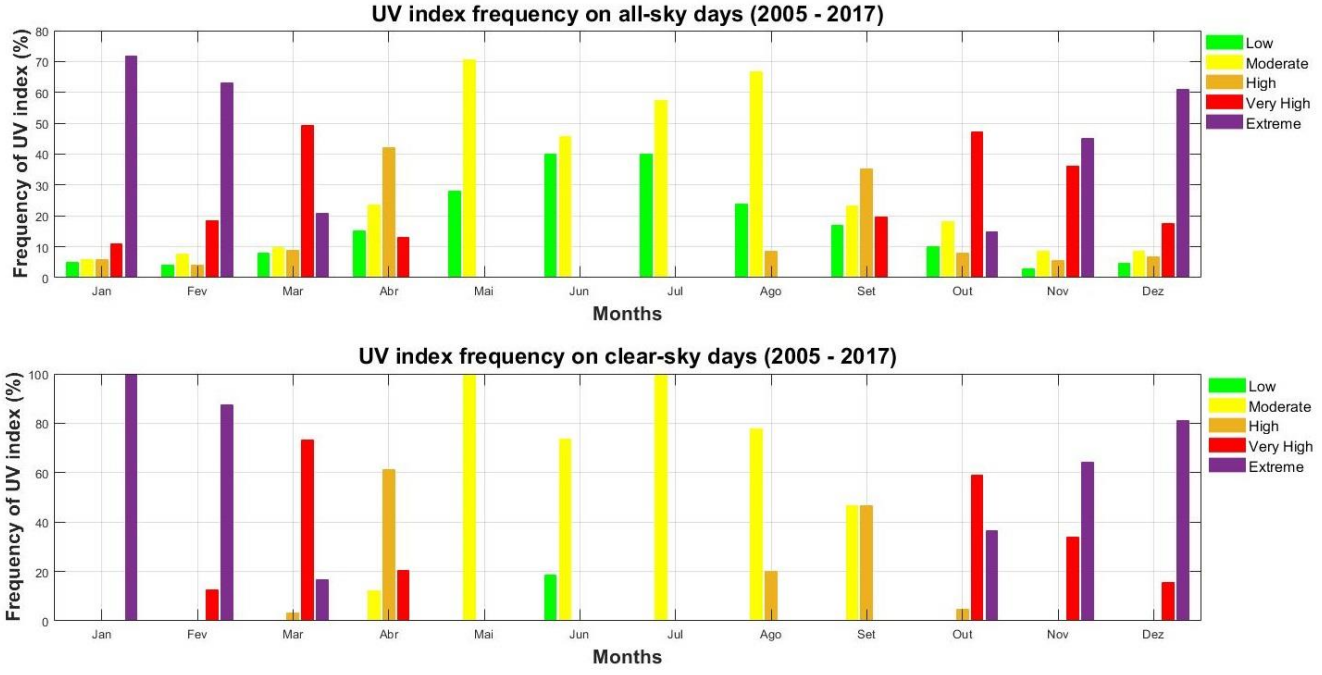


**Figure 7: Frequency of UV index in percentage per month from 2005 to 2017 presented according the scale of colours of UV index, for all-sky condition, plot on top, and clear-sky conditions plot below.**

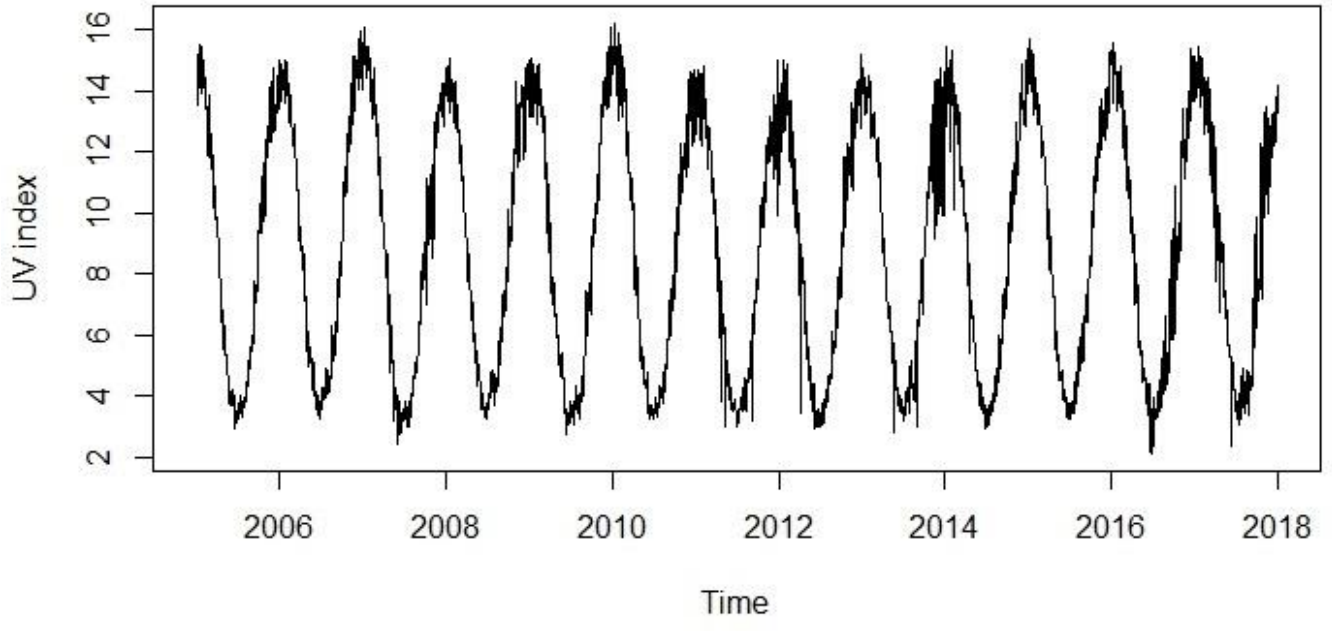


**Figure 8: UV index distribution from Brewer-OMI measured around noon time (local time), from 2005 to 2017.**

https://doi.org/10.5194/egusphere-2023-1474
Preprint. Discussion started: 22 August 2023


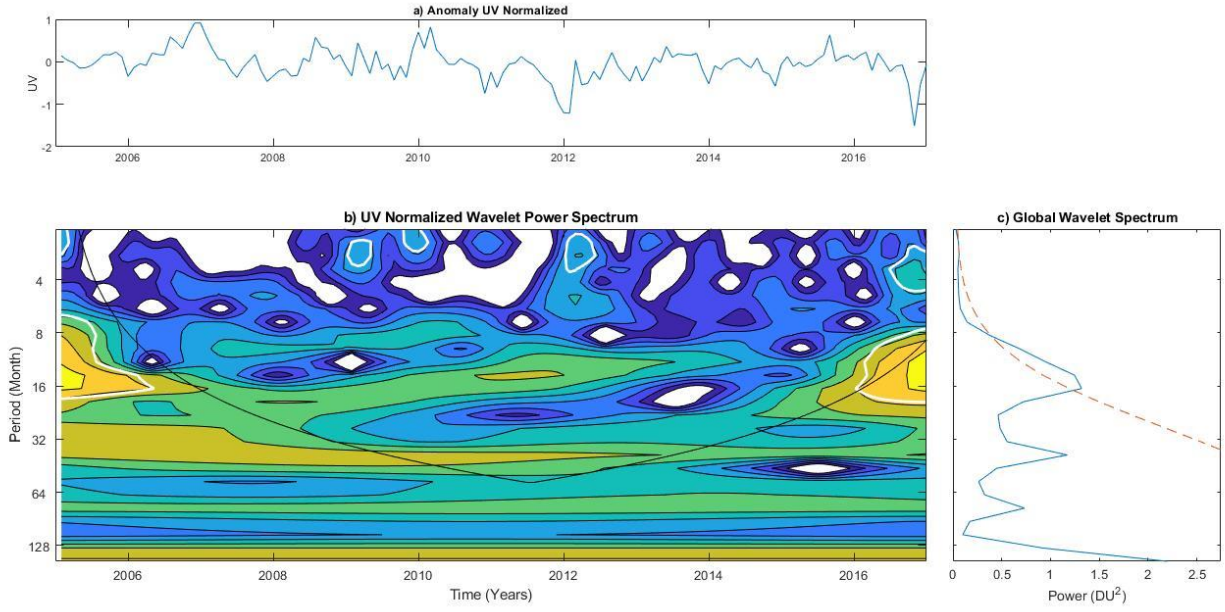


**Figure 9: a) UV index anomaly of UV index data from Brewer-OMI, measured around noon time. b) wavelet power of UV index from Brewer-OMI and c) Global wavelet spectrum of UV index from Brewer-OMI.**

Table 1: Events of secondary effects of AOH considering UV index.

| Date | UV index | Climatological mean UV index | Increase of UV index (%) | Ozone total column (DU) | Climatological mean Ozone (DU) | Decrease of Ozone (%) | Increase of UV index with O3 decrease (%) |
|---|---|---|---|---|---|---|---|
| **29/09/2005** | 9.43 | 6.01 | 56.9 | 261.95 | 296.97 | -11.79 | 4.8 |
| **11/10/2005** | 10.88 | 7.96 | 36.7 | 264.76 | 290.79 | -9.0 | 4.1 |
| **08/10/2007** | 8.65 | 7.96 | 8.7 | 267.57 | 290.79 | -8.0 | 1.1 |
| **28/09/2008** | 9.55 | 6.01 | 58.9 | 253.12 | 296.97 | -14.77 | 4.0 |
| **27/10/2008** | 14.45 | 7.96 | 81.5 | 255.32 | 290.79 | -12.2 | 6.7 |
| **14/09/2012** | 8.44 | 6.01 | 40.38 | 267.79 | 296.97 | -9.83 | 4.1 |
| **22/09/2012** | 8.09 | 6.01 | 34.56 | 277.41 | 296.97 | -6.59 | 5.3 |
| **14/10/2012** | 11.78 | 7.96 | 47.86 | 252.67 | 290.79 | -13.11 | 3.7 |
| **25/08/2016** | 6.15 | 3.98 | 54.52 | 252.85 | 290.06 | -12.83 | 4.3 |

https://doi.org/10.5194/egusphere-2023-1474
Preprint. Discussion started: 22 August 2023


| | | | | | | | |
|---|---|---|---|---|---|---|---|
| 21/10/2016 | 15.02 | 7.96 | 88.7 | 233.29 | 290.79 | -19.8 | 4.5 |

765

Table 2: Events of secondary effects of AOH considering UV-B non-weighted

| **Date** | **UV-B ($W/m^2$)** | **Climatological mean UV-B ($W/m^2$)** | **Increase of UV-B ($W/m^2$) (%)** | **Ozone total column (DU)** | **Climatological mean Ozone (DU)** | **Decrease of Ozone (%)** | **Increase of UV-B with $O_3$ decrease (%)** |
|---|---|---|---|---|---|---|---|
| **29/9/2005** | 1669 | 638 | 161.7 | 261.95 | 296.97 | -11.79 | 13.7 |
| **11/10/2005** | 1885 | 764 | 146.7 | 264.76 | 290.79 | -9.0 | 16.4 |
| **08/10/2007** | 1354 | 764 | 77.2 | 267.57 | 290.79 | -8.0 | 9.7 |
| **28/09/2008** | 1655 | 638 | 159.4 | 253.12 | 296.97 | -14.77 | 10.8 |
| **27/10/2008** | 2480 | 764 | 224.6 | 255.32 | 290.79 | -12.2 | 18.4 |
| **14/09/2012** | 1366 | 638 | 114.1 | 267.79 | 296.97 | -9.83 | 11.6 |
| **22/09/2012** | 1303 | 638 | 104.2 | 277.41 | 296.97 | -6.59 | 15.8 |
| **14/10/2012** | 1886 | 764 | 146.9 | 252.67 | 290.79 | -13.11 | 11.2 |
| **25/08/2016** | 1112 | 417 | 166.7 | 252.85 | 290.06 | -12.83 | 13.0 |
| **21/10/2016** | 2348 | 764 | 207.3 | 233.29 | 290.79 | -19.8 | 10.5 |

770

https://doi.org/10.5194/egusphere-2023-1474
Preprint. Discussion started: 22 August 2023


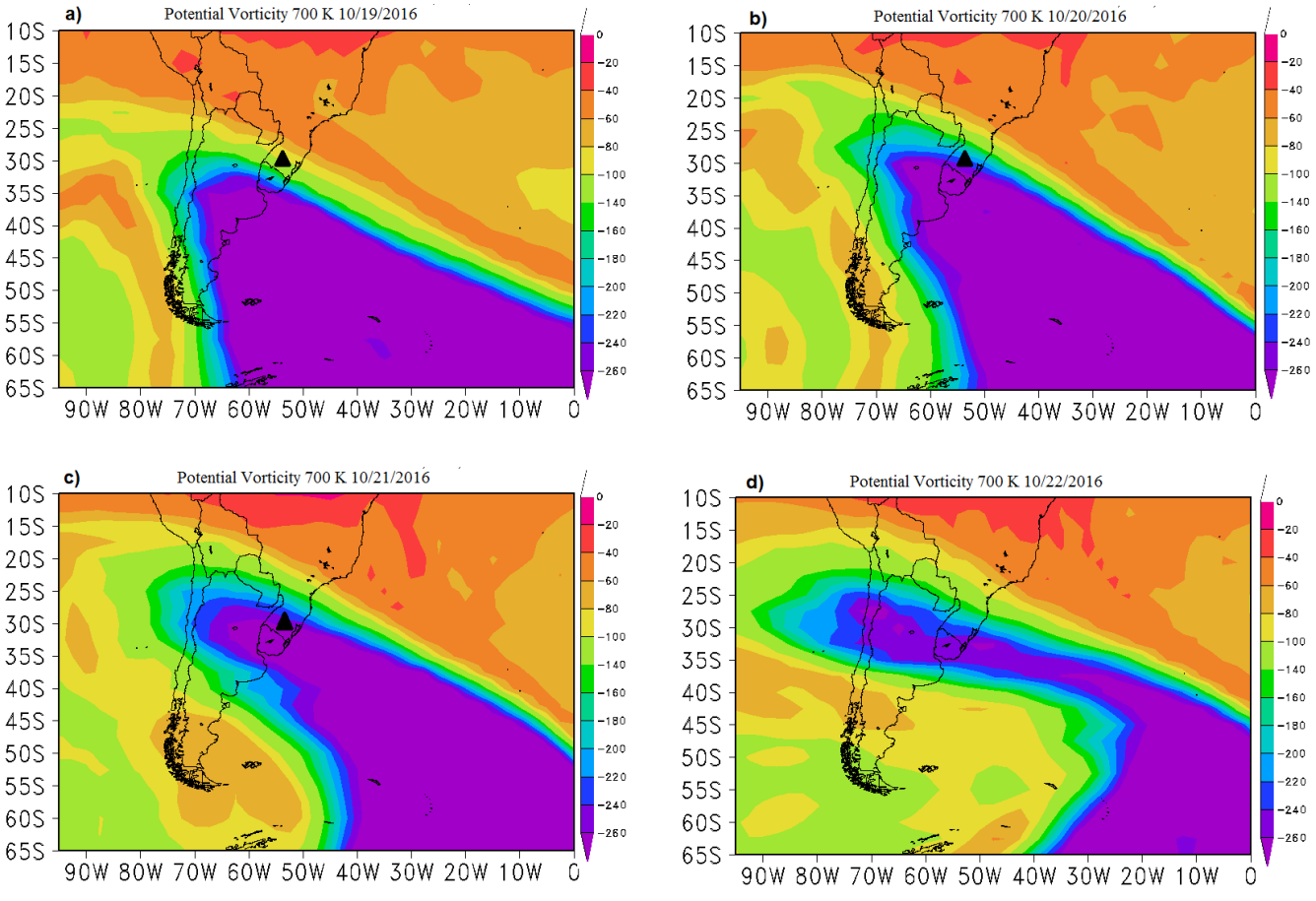


Source: (BITTENCOURT et al., 2018)

**Figure 10: Potential vorticity at potential temperature level of 700 K, on October 19 (a), 20 (b), 21 (c) and 22 (d) 2016 at the region of study (highlighted in a, b and c. The scale of colours varies from 0 to 260.**

775

https://doi.org/10.5194/egusphere-2023-1474
Preprint. Discussion started: 22 August 2023


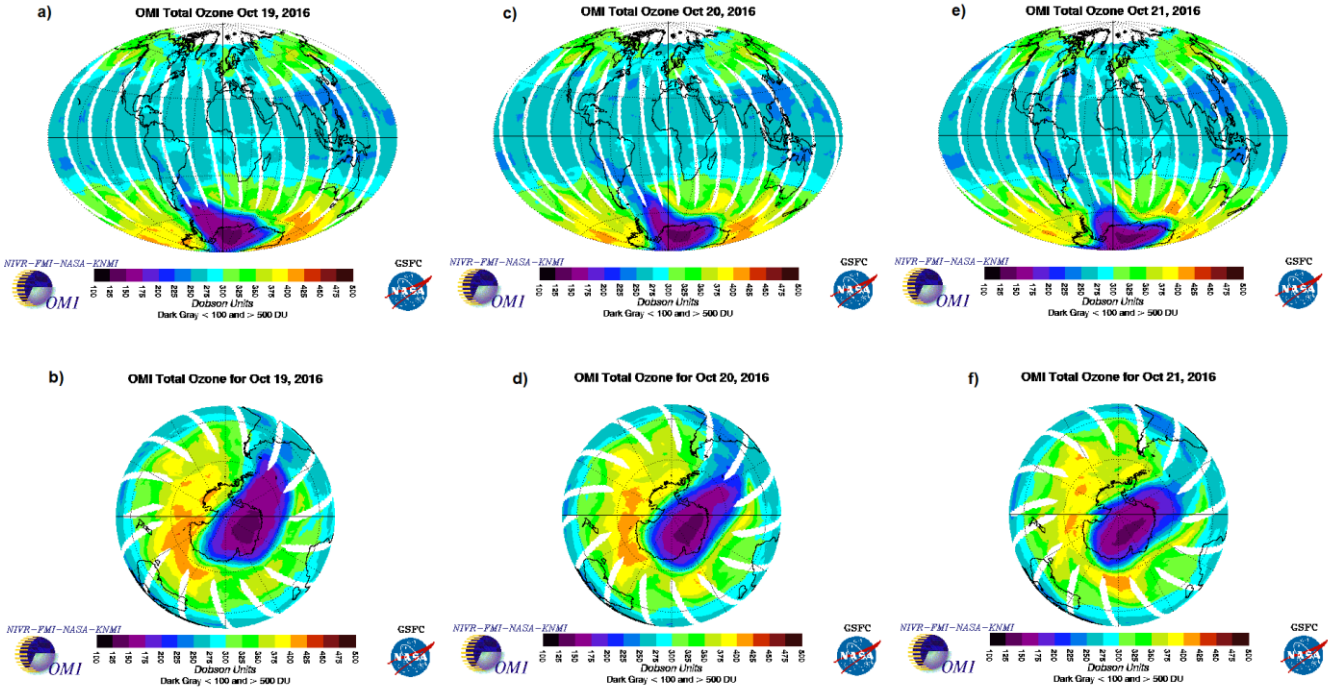


Source: (BITTENCOURT et al., 2018)

**Figure 11: Image of OMI satellite showing ozone total column (Dobson Units) depletion on Antarctic region and its influence over south of Brazil.**

https://doi.org/10.5194/egusphere-2023-1474
Preprint. Discussion started: 22 August 2023


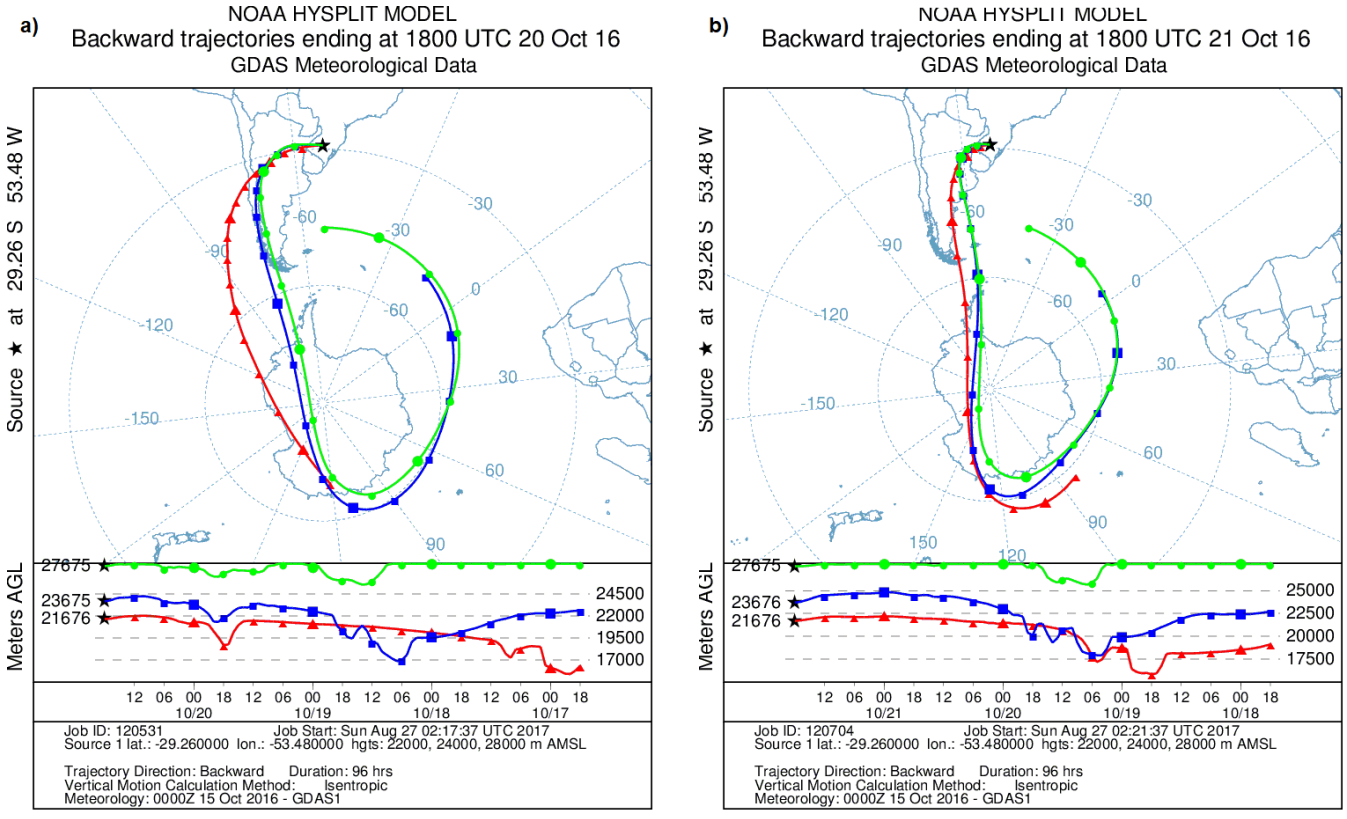


Source: (BITTENCOURT et al., 2018)

**Figure 12: Backward trajectories of HYSPLIT/NOAA model, of poor-ozone air mass reaching the south of Brazil in three different heights 28 km (green), 24 km (blue) and 20 km (red), on October 20 (a) and 21 (b), 2016.**

https://doi.org/10.5194/egusphere-2023-1474
Preprint. Discussion started: 22 August 2023


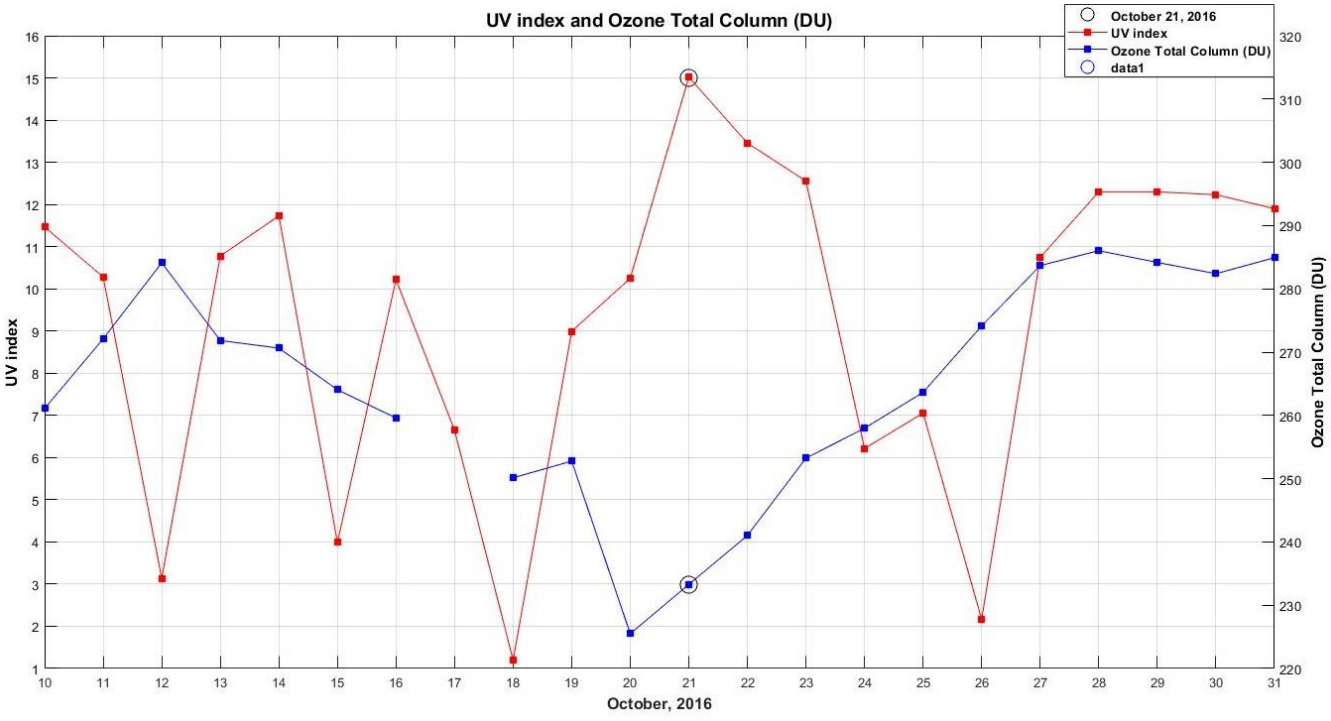


785

**Figure 13: UV index (red doted-line) from Brewer and Ozone total column (Dobson Units) (blue doted-line) from Brewer and OMI, in October, 21 2016 (black circle)**

https://doi.org/10.5194/egusphere-2023-1474
Preprint. Discussion started: 22 August 2023


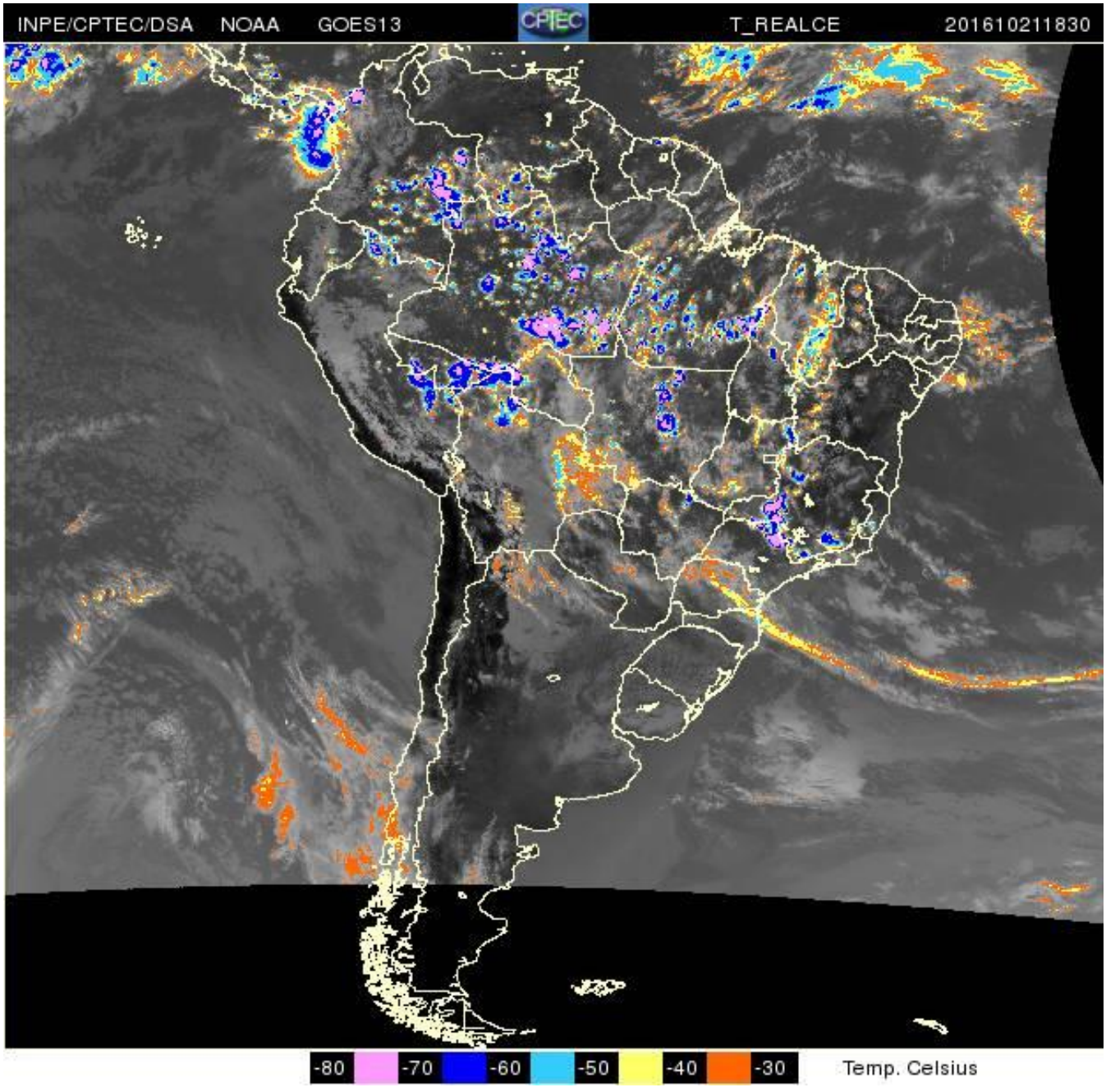


790 Source: CPTEC/INPE, 2017.

**Figure 14: Satellite image GOES 13, infrared thermal channel at 15 hours, local time, on October, 20 2016.**